Supporting Information

Tuning Colourimetric Indicator Displacement Assays for Naked-Eye Sensing of Pyrophosphate in Aqueous Media†

*Xuejian Liu,‡ Huy Tien Ngo,‡ Zijun Ge, Stephen J. Butler and Katrina A. Jolliffe**

School of Chemistry, The University of Sydney, Sydney, NSW 2006, Australia.

E-mail: kate.jolliffe@sydney.edu.au; Fax: +61 2 9351 3329; Tel: +61 2 9351 2297

‡These authors contributed equally

Contents

1. Synthesis

General. Optical rotations were performed using a Perkin Elmer Model 341 polarimeter using the indicated spectroscopic grade solvents. ^{1}H NMR spectra were recorded using a Bruker Avance III 500 at a frequency of 500.13 MHz, a Bruker Avance DPX 400 at a frequency of 400.13 MHz or a Bruker Avance DPX 300 at a frequency of 300.13 MHz and are reported as parts per million (ppm) with $CDCl_3$ (δ_H 7.26 ppm) or CD_3OD (δ_H 3.31 ppm) as an internal reference. The data are reported as chemical shift (δ), multiplicity (br = broad, s = singlet, d = doublet, t = triplet, m = multiplet), coupling constant (*J* Hz) and relative integral. ^{13}C NMR spectra were recorded using a Bruker Avance III 500 at a frequency of 125.76 MHz, a Bruker Avance DPX 400 at a frequency of 100.61 MHz or a Bruker Avance DPX 300 at a frequency of 75.47 MHz and are reported as parts per million (ppm) with $CDCl_3$ (δ_C 77.16 ppm) or CD_3OD (δ_C 49.00 ppm) as an internal reference. ^{31}P{^{1}H} NMR spectra were recorded using a Bruker Avance III 500 at a frequency of 202.46 MHz and are reported as parts per million (ppm) relative to 85% H_3PO_4 in D_2O (0 ppm). High resolution ESI spectra were recorded on a Bruker BioApex Fourier Transform Ion Cyclotron Resonance mass spectrometer (FTICR) with an Analytica ESI source, operating at 4.7 T or a Bruker Daltonics Apex Ultra FTICR with an Apollo Dual source, operating at 7T. Compounds **1** and **3** were synthesized using modified literature procedures.[1] Compounds **2, 4-8** have not been reported previously and full characterization is provided (except for compound **8** where a ^{13}C NMR spectrum could not be obtained due to lack of material).

Solid-phase peptide synthesis of linear peptides and macrolactamisation

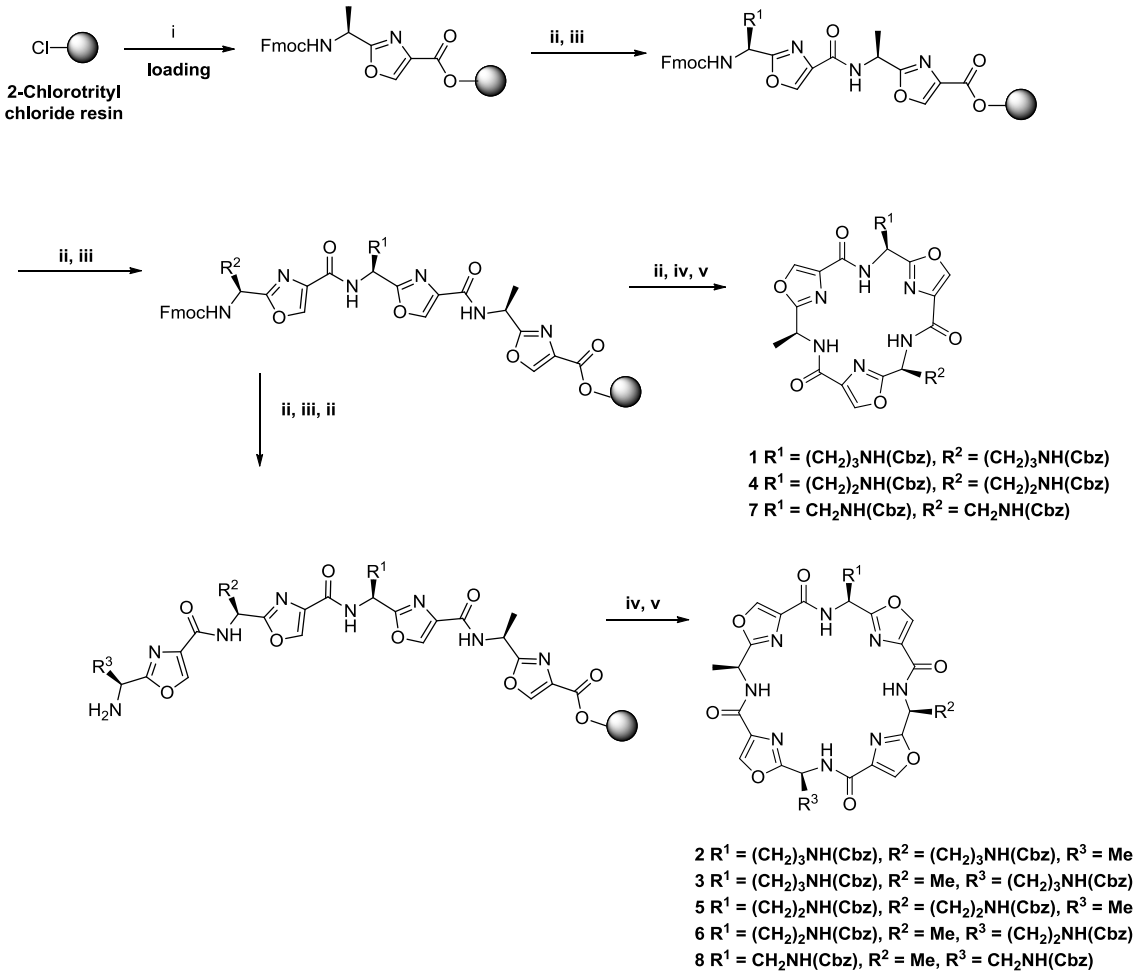

Scheme S1. Cyclic peptide synthesis conditions: (i) Fmoc-Ala-Oxz(Ser)-OH (1.7 equiv), Hünig's base (3 equiv), DCM-DMF (9:1 v/v), 3 d; (ii) 10% v/v piperidine in DMF, 3 x 10 min; (iii) Fmoc-protected oxazole-based amino acids (1.2 equiv), HATU (1.2 equiv), NMM (2 equiv), DMF, 50 min; (iv) hexafluoroisopropanol-dichloromethane (1:4 v/v), 4 x 10 min; (v) DMTMM (1.3 equiv), Hünig's base (3 equiv), DMF (0.05 M), 24 h, rt, preparative HPLC purification.

General procedures for SPPS

Loading of Fmoc-protected oxazole-based amino acid onto 2-chlorotrityl chloride resin and capping. 2-chlorotrityl chloride resin (resin capacity 1.3 mmol g^{-1}) was swollen in anhydrous dichloromethane for 1 h in a sinter-fitted syringe. After filtering off the resin, a solution of Fmoc-Ala-Oxz(Ser)-OH (1.7 equiv. relative to resin capacity) and Hünig's base (3 equiv. relative to resin capacity) in anhydrous dichloromethane-DMF (9:1 v/v, 0.2 M) was added. Agitated at rt for 3d, the resin was drained and treated with a solution of methanol-Hünig's base-dichloromethane (2:1:17 v/v/v, 3 x 5 mL x 10 min). The resin was then washed with DMF (3 x 6 mL), dichloromethane (3 x 6 mL) and diethyl ether (3 x 6 mL) before being dried under reduced pressure overnight. The resin loading was calculated to be 1.15 mmol g^{-1} according to gravimetric measurements.

Fmoc deprotection. The resin-bound peptide was treated with a solution of 10% piperidine in DMF (3 x 5 mL x 10 min) and subsequently filtered off and washed with DMF (3 x 5 mL), dichloromethane (3 x 5 mL) and DMF (3 x 5 mL) to give the free amine.

Solid phase peptide coupling. A solution of Fmoc-protected oxazole-based amino acid (1.2 equiv. relative to loading), NMM (2 equiv. relative to loading), HATU (1.2 equiv. relative to loading) was added to the reaction vessel. The resulting suspension was shaken at rt for 50 min and then the resin was drained and washed with DMF (3 x 5 mL), dichloromethane (3 x 5 mL) and DMF (3 x 5 mL).

Peptide cleavage from resin. After the coupling, the resin was washed with DMF (5 x 5 mL), CH_2Cl_2 (10 x 5 mL). Then the resin was treated with a solution of hexafluoroisopropanol- CH_2Cl_2 (1:4 v/v, 4 x 6 mL x 10 min). Afterwards, the resin was washed with CH_2Cl_2 (5 x 5 mL). All solutions were combined and evaporated to give the crude linear peptide. Yields: 95 % - 100%.

Macrolactamisation. A solution of the crude linear peptide (1 equiv.) in DMF (0.05 M) was treated with DMTMM (1.3 equiv.) and Hunig's base (3 equiv.) and the resulting mixture was stirred at rt for 16 h. Concentrated and the residue was then partitioned between water (15 mL) and chloroform-isopropanol (3 : 1 v/v, 50 mL). The aqueous phase was extracted again with chloroform-isopropanol (3:1 v/v, 7 x 50 mL), the combined organic fractions were evaporated to give the crude cyclic peptide which was then purified by preparative RP-HPLC [gradient of 10% to 60% acetonitrile (0.1% TFA) in water (0.1% TFA) over 60 min] to afford the desired product as a colorless solid. Yields: 48 % - 53%.

General procedures for functionalization of cyclic peptide side-chains and synthesis of 1•Zn_2 - 8•Zn_2

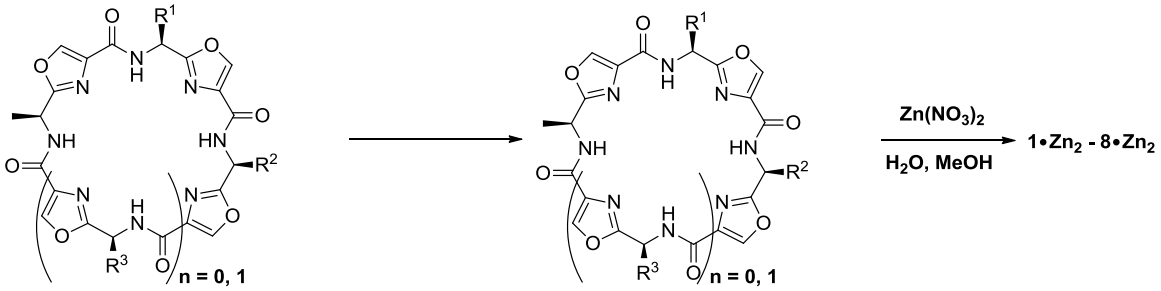

1 $R^1 = (CH_2)_3NH(Cbz)$, $R^2 = (CH_2)_3NH(Cbz)$, n = 0	1 $R^1 = (CH_2)_3N(Dpa)$, $R^2 = (CH_2)_3N(Dpa)$, n = 0
2 $R^1 = (CH_2)_3NH(Cbz)$, $R^2 = (CH_2)_3NH(Cbz)$, R^3 = Me, n = 1	2 $R^1 = (CH_2)_3N(Dpa)$, $R^2 = (CH_2)_3N(Dpa)$, R^3 = Me, n = 1
3 $R^1 = (CH_2)_3NH(Cbz)$, R^2 = Me, $R^3 = (CH_2)_3NH(Cbz)$, n = 1	3 $R^1 = (CH_2)_3N(Dpa)$, R^2 = Me, $R^3 = (CH_2)_3N(Dpa)$, n = 1
4 $R^1 = (CH_2)_2NH(Cbz)$, $R^2 = (CH_2)_2NH(Cbz)$, n = 0	4 $R^1 = (CH_2)_2N(Dpa)$, $R^2 = (CH_2)_2N(Dpa)$, n = 0
5 $R^1 = (CH_2)_2NH(Cbz)$, $R^2 = (CH_2)_2NH(Cbz)$, R^3 = Me, n = 1	5 $R^1 = (CH_2)_2N(Dpa)$, $R^2 = (CH_2)_2N(Dpa)$, R^3 = Me, n = 1
6 $R^1 = (CH_2)_2NH(Cbz)$, R^2 = Me, $R^3 = (CH_2)_2NH(Cbz)$, n = 1	6 $R^1 = (CH_2)_2N(Dpa)$, R^2 = Me, $R^3 = (CH_2)_2N(Dpa)$, n = 1
7 $R^1 = CH_2NH(Cbz)$, $R^2 = CH_2NH(Cbz)$, n = 0	7 $R^1 = CH_2N(Dpa)$, $R^2 = CH_2N(Dpa)$, n = 0
8 $R^1 = CH_2NH(Cbz)$, R^2 = Me, $R^3 = CH_2NH(Cbz)$, n = 1	8 $R^1 = CH_2N(Dpa)$, R^2 = Me, $R^3 = CH_2N(Dpa)$, n = 1

Scheme S2 Side chain functionalisation of cyclic peptides and synthesis of **1•Zn_2 - 8•Zn_2**

Step 1. A solution of hydrogen bromide in acetic acid (33% v/v, 3.0 mL) was added to the cyclic peptide (0.07 mmol) and stirred at rt for 2h. The reaction mixture was treated with anhydrous ether (80 mL) to give a precipitate which was collected by centrifuge. The obtained dihydrobromide salt was then partitioned between chloroform-isopropanol (3 : 1 v/v, 20 mL) and NaOH (0.2 M, pH 8). The aqueous phase was extracted with chloroform-isopropanol (3 : 1 v/v, 9 x 20 mL). The combined organic fractions were dried ($MgSO_4$) and the solvent was removed under reduced pressure to give the free diamine.

Step 2. To a stirred solution of the free diamine in anhydrous DMF (5.0 mL) was added 2-pyridinecarboxaldehyde (25 equiv.) and sodium triacetoxyborohydride (25 equiv.). The resulting mixture was evaccuated and refilled with nitrogen three times and stirred at rt for 16 h. Then the mixture was concentrated and treated with NaOH (0.1 M, pH 8). The aqueous phase was extracted with chloroform-isopropanol (3 : 1 v/v, 10 x 20 mL). The combined organic fractions was dried ($MgSO_4$) and the solvent was evaporated to give the crude cyclic peptide which was then purified by RP-HPLC [gradient of 0% to 45% acetonitrile (0.02% ammonium) in water (0.02% ammonium) over 60 min] to afford the desired product. Yields: 30% - 70%.

Step 3. To a solution of cyclic peptide in methanol (3.0 mL) was added an aqueous solution of zinc nitrate (0.03 M, 2.0 equiv.). The mixture was stirred at rt for 5 min and subsequent evaporation of the solvent and dried to afford the bis[zinc(II)] complex **1•Zn$_2$ - 8•Zn$_2$** as a colourless solid (quant.).

Cyclo[Ala-Oxz(Ser)-Orn(DPA)-Oxz(Ser)-Orn(DPA)-Oxz(Ser)] (1)

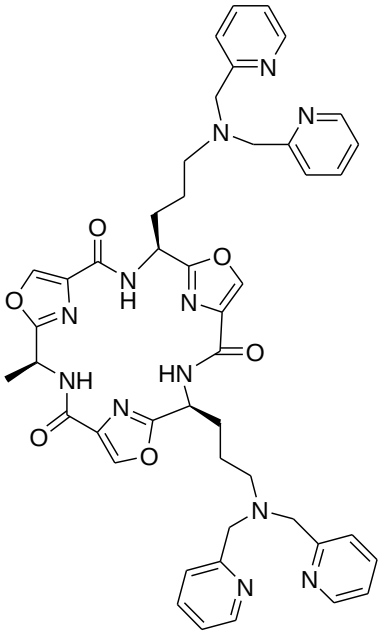

Yield 61%; $[\alpha]_D^{20}$ = -22.2 (*c* 0.3 MeOH) ; [lit.[2] $[\alpha]_D^{25}$ = -18.8 (*c* 0.68 MeOH)]

Cyclo[Ala-Oxz(Ser)]$_2$-[Orn(DPA)-Oxz(Ser)]$_2$ (2)

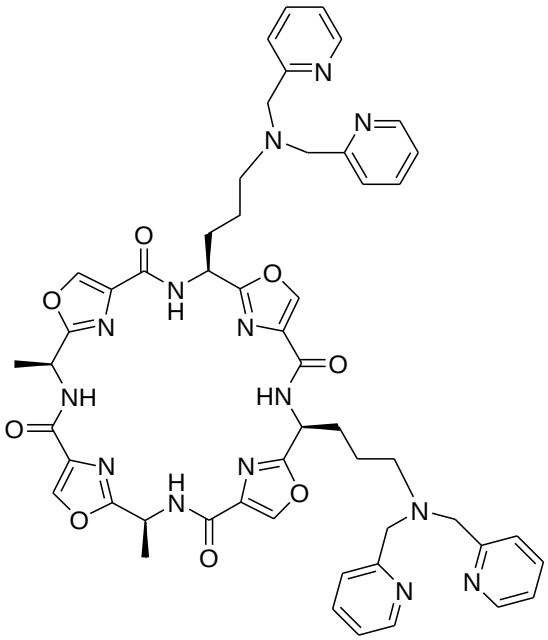

Yield 52%; $[\alpha]_D^{20}$ = -97.1 (*c* 0.1 MeOH); ^{1}H NMR (400 MHz, CD_3OD): δ 8.41 (d, *J* = 4.4 Hz, 4H), 8.35 (m, 4H), 7.78 (m, 4H), 7.60 (m, 4H), 7.25 (m, 4H), 5.47 (m, 2H), 5.28 (m, 2H), 3.77 (m, 8H), 2.60 (t, *J* = 6.8 Hz, 4H), 2.12 (m, 2H), 1.96 (m, 2H), 1.67 (d, *J* = 2.4 Hz, 3H), 1.65 (d, *J* = 2.4 Hz, 3H), 1.65 (m, 4H); ^{13}C NMR (100 MHz, CD_3OD): δ 166.1, 165.6, 160.6, 149.5, 149.4, 144.0, 143.9, 138.6, 136.8, 124.9, 123.8, 61.2, 54.8, 43.7, 43.6, 31.7, 24.3, 19.1; HRMS (ESI) calcd. for $C_{52}H_{55}N_{14}O_8$ $[M+H]^+$ 1003.4327, found 1003.4322.

Cyclo[Ala-Oxz(Ser)-Orn(DPA)-Oxz(Ser)]$_2$ (3)

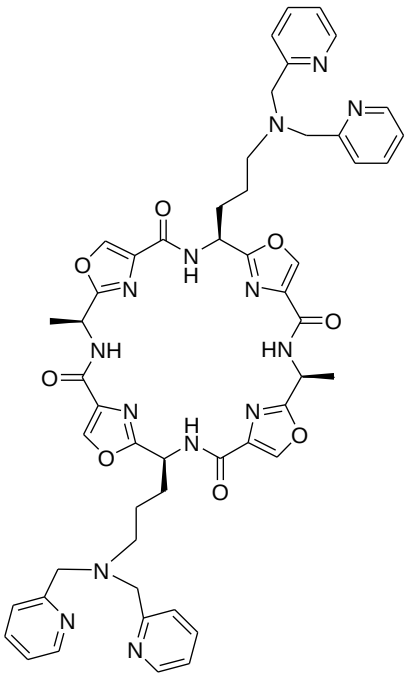

Yield 51%; $[\alpha]_D^{20}$ = -110.5 (*c* 0.20 MeOH); [lit.[3] $[\alpha]_D^{20}$ = -86.8 (*c* 0.65 MeOH)]

Cyclo[Ala-Oxz(Ser)-Dab(DPA)-Oxz(Ser)-Dab(DPA)-Oxz(Ser)] (4)

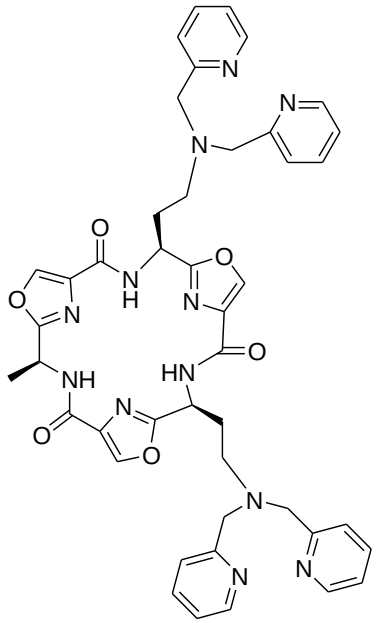

Yield 70%; $[\alpha]_D^{20}$ = -6.0 (*c* 0.2 MeOH); ^{1}H NMR (500 MHz, CD_3OD): δ 8.42 (s, 1H),), 8.40 (m, 4H), 8.38 (s, 1H), 8.28 (s, 1H), 7.75 (m, 4H), 7.58 (m, 4H), 7.24 (m, 4H), 5.27 (m, 2H), 5.14 (m, 1H), 3.85 (m, 4H), 3.70 (m, 4H), 2.66 (m, 4H), 2.56 (m, 4H), 2.30 (m, 4H), 1.66 (d, *J* = 7.0 Hz, 3H); ^{13}C NMR (125 MHz, CD_3OD): δ 165.7, 164.9, 164.8, 161.1, 161.0, 160.9, 149.4, 143.6, 138.6, 136.1, 125.1, 123.8, 60.9, 50.5, 48.6, 45.8, 32.3, 32.2, 20.6; HRMS (ESI) calcd. for $C_{44}H_{44}N_{12}O_6Na$ $[M+Na]^+$ 859.3404, found 859.3399.

Cyclo[Ala-Oxz(Ser)]$_2$-[Dab(DPA)-Oxz(Ser)]$_2$ (5)

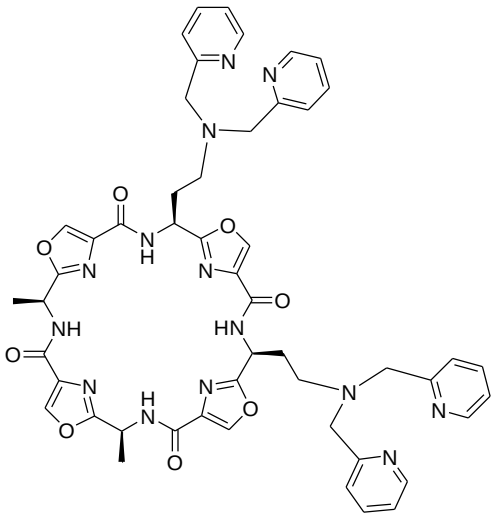

Yield 42%; $[\alpha]_D^{20}$ = -84.9 (*c* 0.2 MeOH); ^{1}H NMR (300 MHz, CD_3OD): δ 8.38 (m, 5H), 8.33 (s, 1H), 8.28 (s, 1H), 8.25 (s, 1H), 7.72 (m, 4H), 7.63 (m, 4H), 7.24 (m, 4H), 5.62 (m, 2H), 5.46 (m, 2H), 3.76 (m, 8H), 2.68 (m, 4H), 2.16 (m, 2H), 2.33 (m, 2H), 1.64 (d, *J* = 7.2 Hz, 6H); ^{13}C NMR (75 MHz, CD_3OD): δ 166.3, 165.9, 165.6, 165.2, 162.2, 161.9, 161.8, 149.4, 143.9, 138.8, 136.8,

125.1, 123.8, 61.1, 51.2, 45.7, 45.5, 43.7, 43.6, 31.5, 30.8, 19.0; HRMS (ESI) calcd. for $C_{50}H_{51}N_{14}O_8$ $[M+H]^+$ 975.4014, found 975.4001.

Cyclo[Ala-Oxz(Ser)-Dab(DPA)-Oxz(Ser)]$_2$ (6)

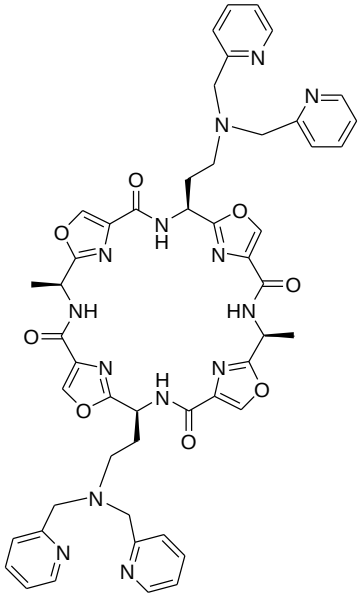

Yield 45%; $[\alpha]_D^{20}$ = -82.8 (*c* 0.2 MeOH); ^{1}H NMR (300 MHz, CD_3OD): δ 8.38 (m, 3H), 8.35 (s, 2H), 8.26 (s, 2H),7.76 (m, 4H), 7.60 (m, 5H), 7.23 (m, 4H), 5.63 (t, *J* = 7.2 Hz, 2H), 5.44 (m, 2H), 3.77 (m, 8H), 2.64 (m, 4H), 2.37 (m, 2H), 2.23 (m, 2H), 1.61 (d, *J* = 7.2 Hz, 6H); ^{13}C NMR (75 MHz, CD_3OD): δ 166.2, 165.0,162.0, 161.8, 160.3, 149.3, 143.9, 138.8, 136.8, 125.1, 123.8, 61.1, 51.0, 45.4, 43.7, 31.2, 19.2; HRMS (ESI) calcd. for $C_{50}H_{51}N_{14}O_8$ $[M+H]^+$ 975.4014, found 975.4001.

Cyclo[Ala-Oxz(Ser)-Dap(DPA)-Oxz(Ser)-Dap(DPA)-Oxz(Ser)] (7)

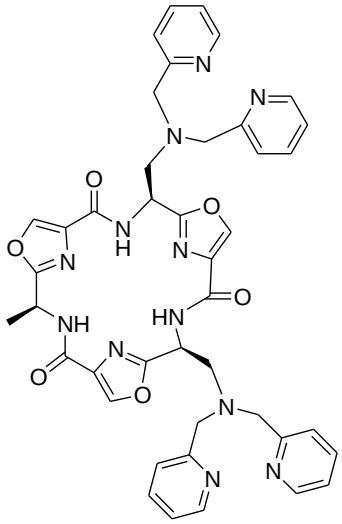

Yield 67%; $[\alpha]_D^{20}$ = +23.2 (*c* 0.4 MeOH); ^{1}H NMR (300 MHz, CD_3OD): δ 8.29 (m, 7H), 7.60 (m, 4H), 7.33 (m, 4H), 7.10 (m, 4H), 5.19 (m, 3H), 3.74 (m, 8H), 3.11 (m, 4H), 1.53 (d, *J* = 6.9 Hz,

3H); ^{13}C NMR (75 MHz, CD_3OD): δ 165.7, 164.6, 164.4, 160.1, 160.0, 149.6, 149.5, 143.7, 143.6, 143.5, 138.5, 136.3, 136.1, 136.0, 124.9, 124.8, 123.9, 123.8, 61.9, 61.7, 58.6, 58.3, 45.6, 20.7; HRMS (ESI) calcd. for $C_{42}H_{41}N_{12}O_6$ $[M+H]^+$ 809.3272, found 809.3267.

Cyclo[Ala-Oxz(Ser)-Dap(DPA)-Oxz(Ser)]$_2$ (8)

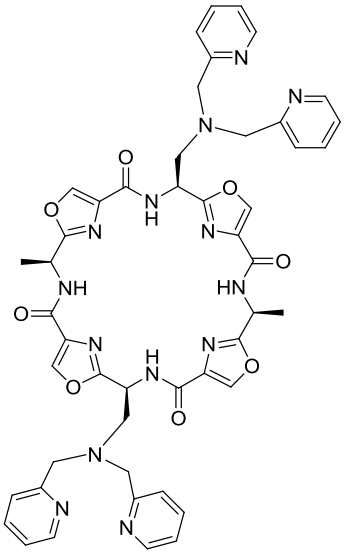

Yield 30%; ^{1}H NMR (300 MHz, CD_3OD): δ 8.47 (m, 7H), 7.71 (m, 4H), 7.35 (m, 9H), 5.50 (m, 4H), 3.93 (s, 8H), 3.24 (m, 4H), 1.66 (d, *J* = 6.9 Hz, 3H); HRMS (ESI) calcd. for $C_{48}H_{47}N_{14}O_8$ $[M+H]^+$ 947.3012, found 947.3013.

^{1}H and ^{13}C NMR spectra of compound 2

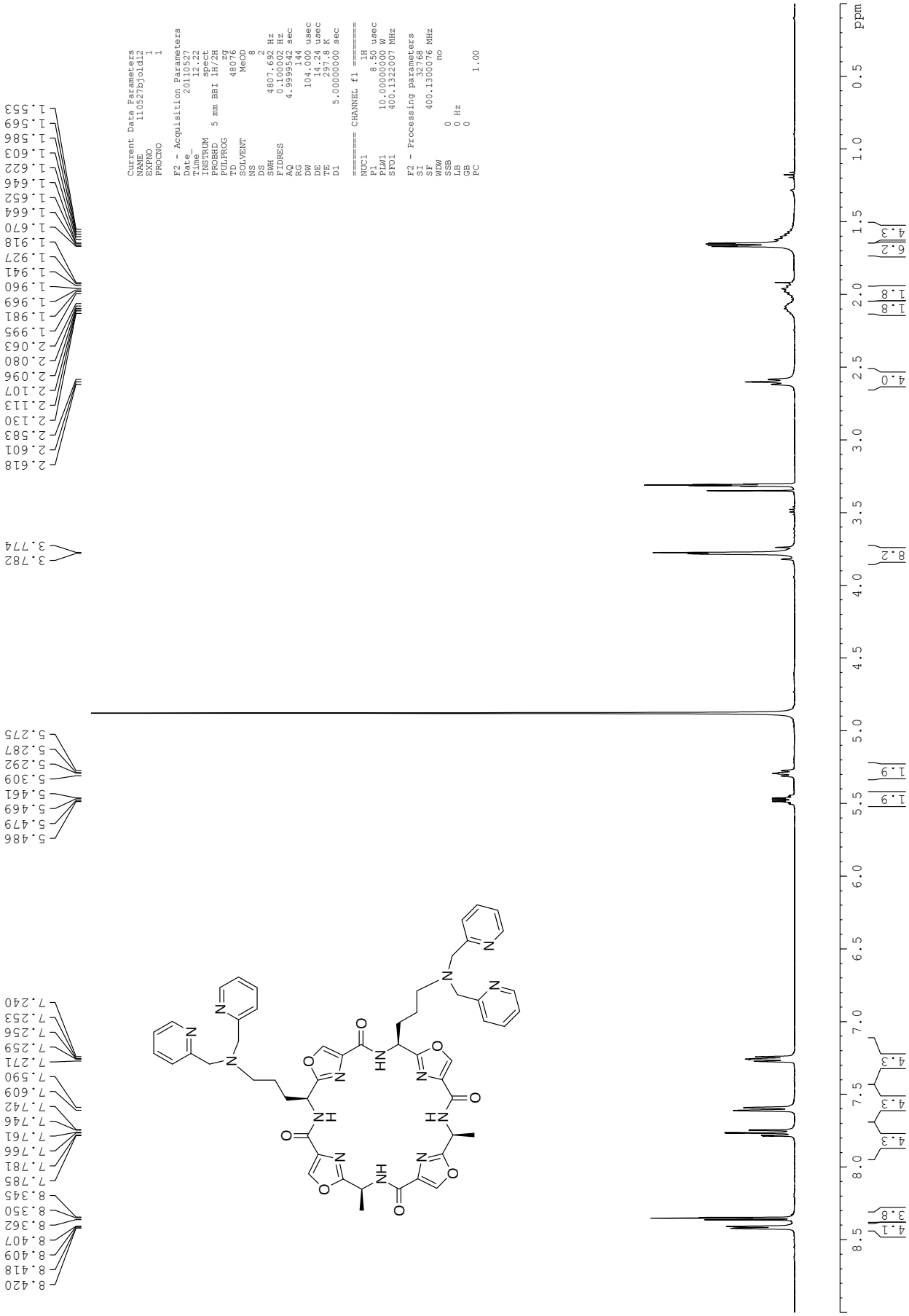

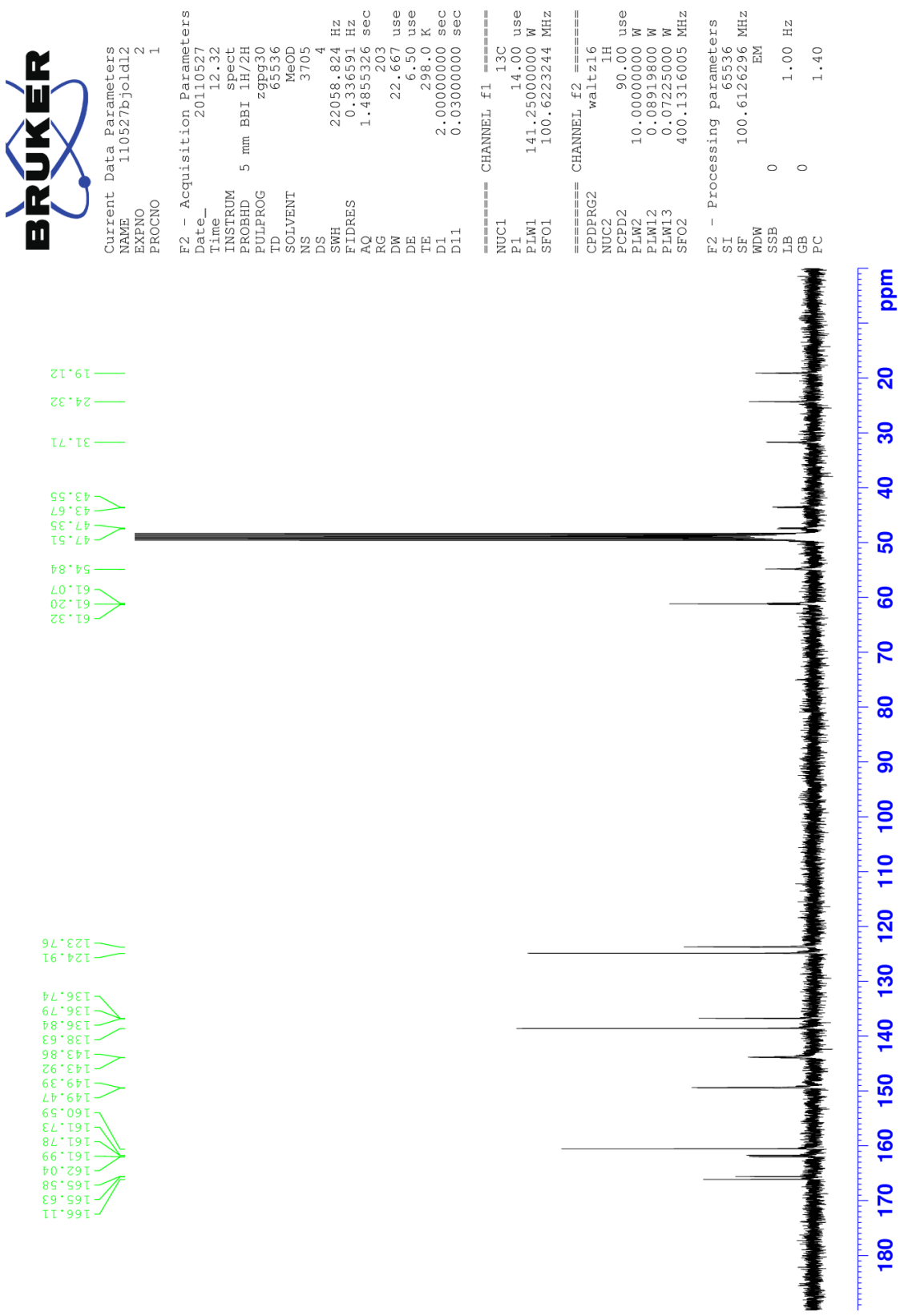
Current Data Parameters
NAME 110527bjoldl2
EXPNO 2
PROCNO 1
F2 - Acquisition Parameters
Date_ 20110527
Time 12.32
INSTRUM spect
PROBHD 5 mm BBI 1H/2H
PULPROG zgpg30
TD 65536
SOLVENT MeOD
NS 3705
DS 4
SWH 22058.824 Hz
FIDRES 0.336591 Hz
AQ 1.4855326 sec
RG 203
DW 22.667 use
DE 6.50 use
TE 298.0 K
D1 2.00000000 sec
D11 0.03000000 sec
======== CHANNEL f1 ========
NUC1 13C
P1 14.00 use
PLW1 141.25000000 W
SFO1 100.6223244 MHz
======== CHANNEL f2 ========
CPDPRG2 waltz16
NUC2 1H
PCPD2 90.00 use
PLW2 10.00000000 W
PLW12 0.08919800 W
PLW13 0.07225000 W
SFO2 400.1316005 MHz
F2 - Processing parameters
SI 65536
SF 100.6126296 MHz
WDW EM
SSB 0
LB 1.00 Hz
GB 0
PC 1.40
19.12
24.32
31.71
43.55
43.67
47.35
47.51
54.84
61.07
61.20
61.32
123.76
124.91
136.74
136.79
136.84
138.63
143.86
143.92
149.39
149.47
160.59
161.73
161.78
161.99
162.04
165.58
165.63
166.11
ppm

^{1}H and ^{13}C NMR spectra of compound 4

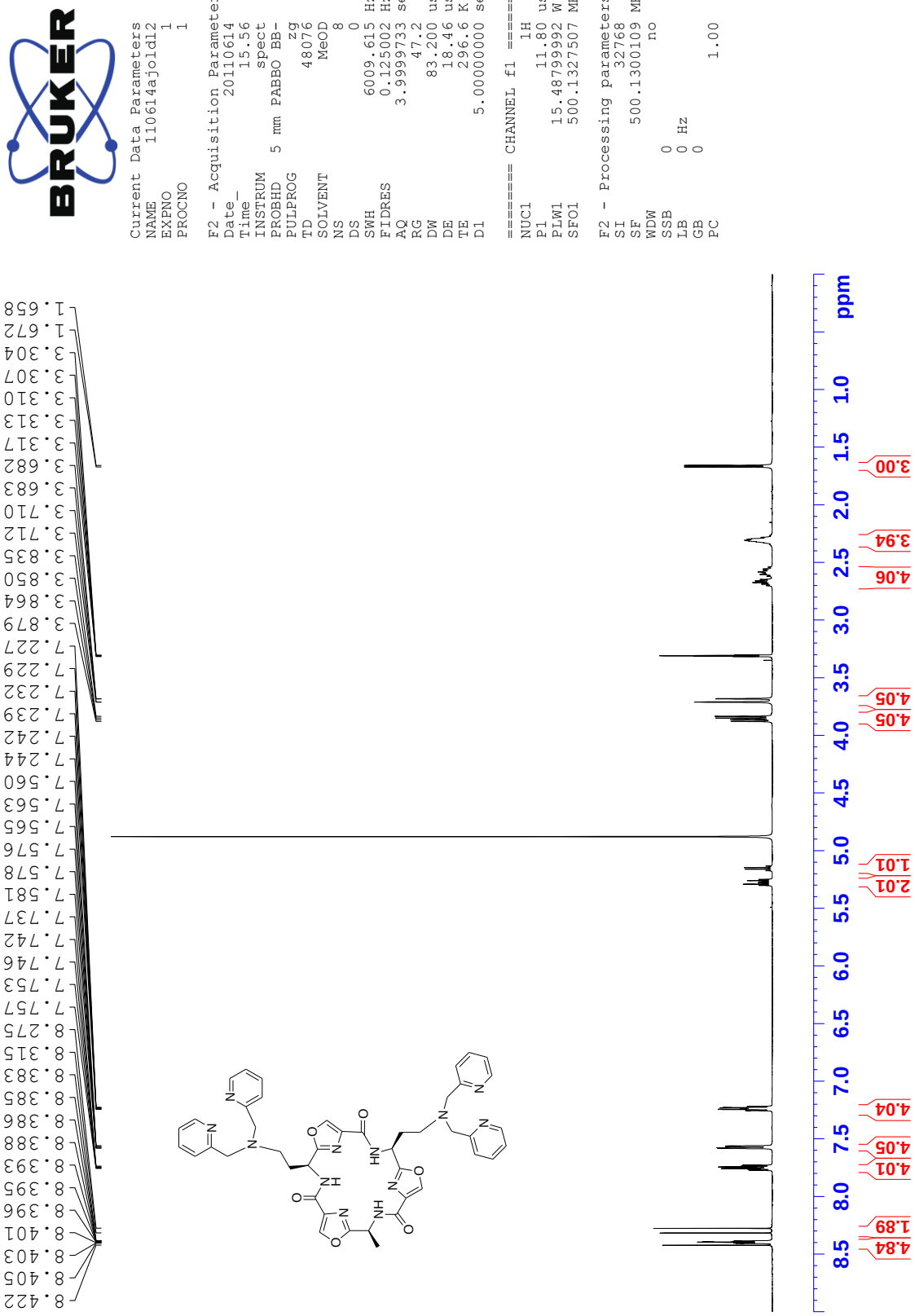

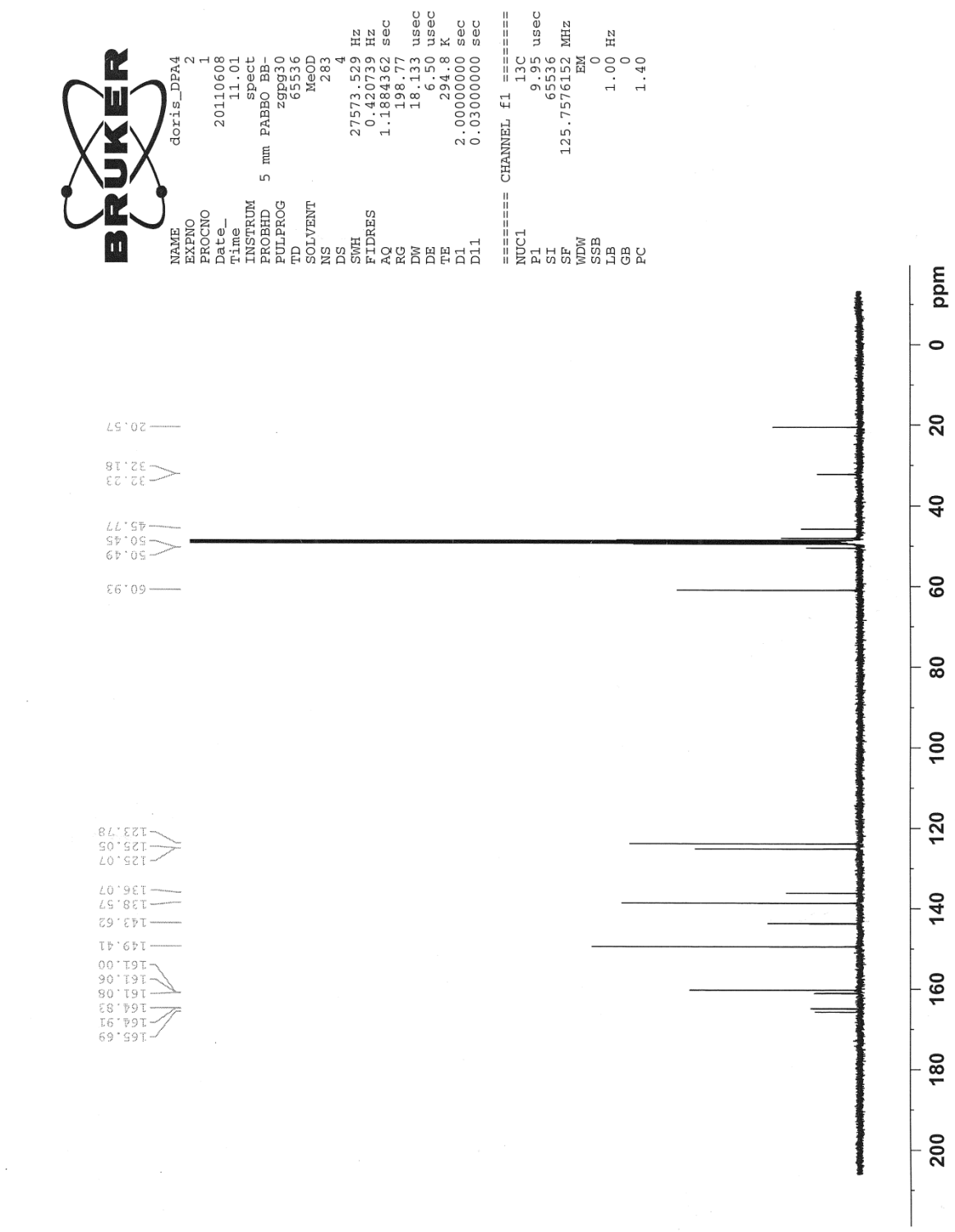

^{1}H and ^{13}C NMR spectra of compound 5

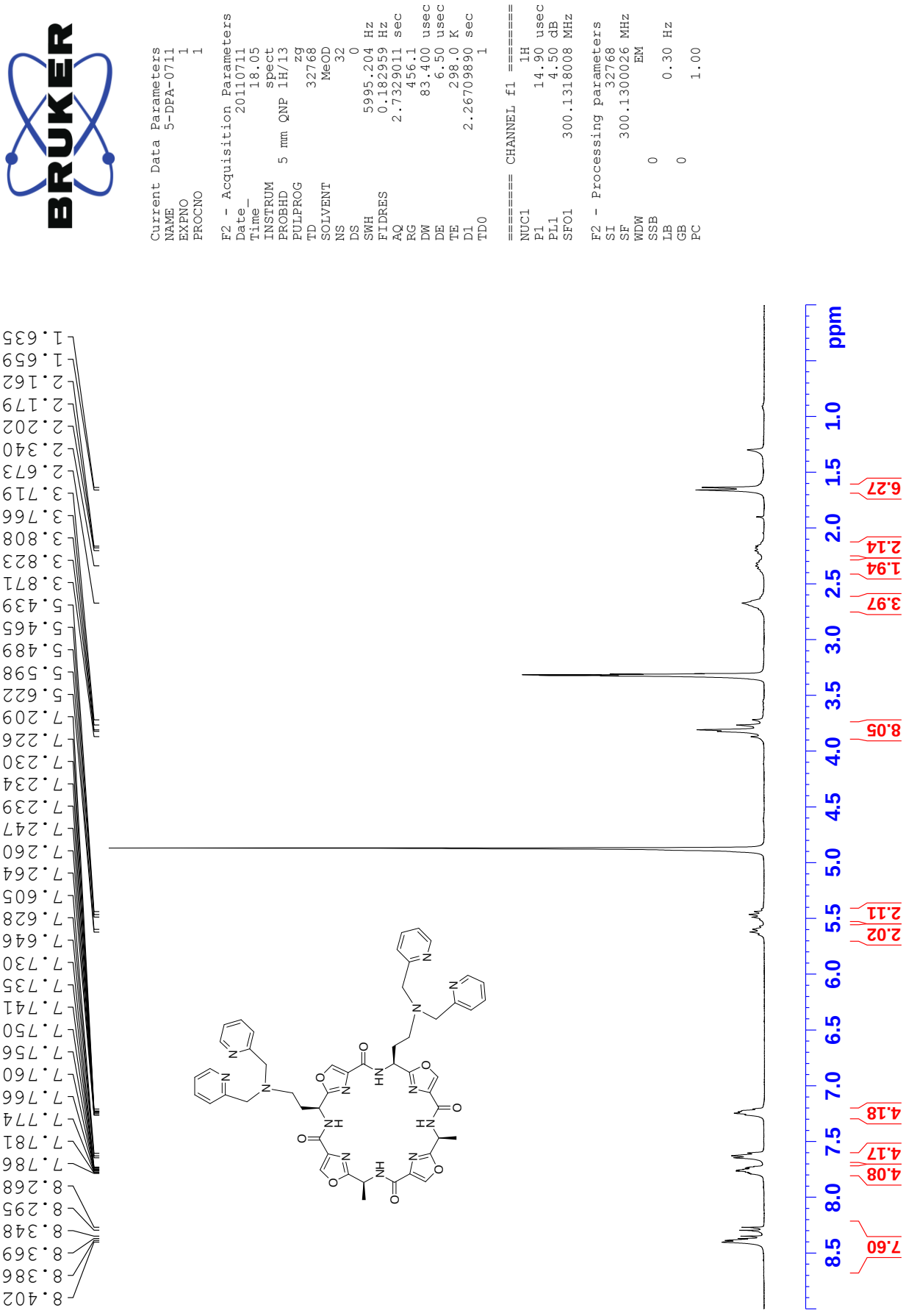

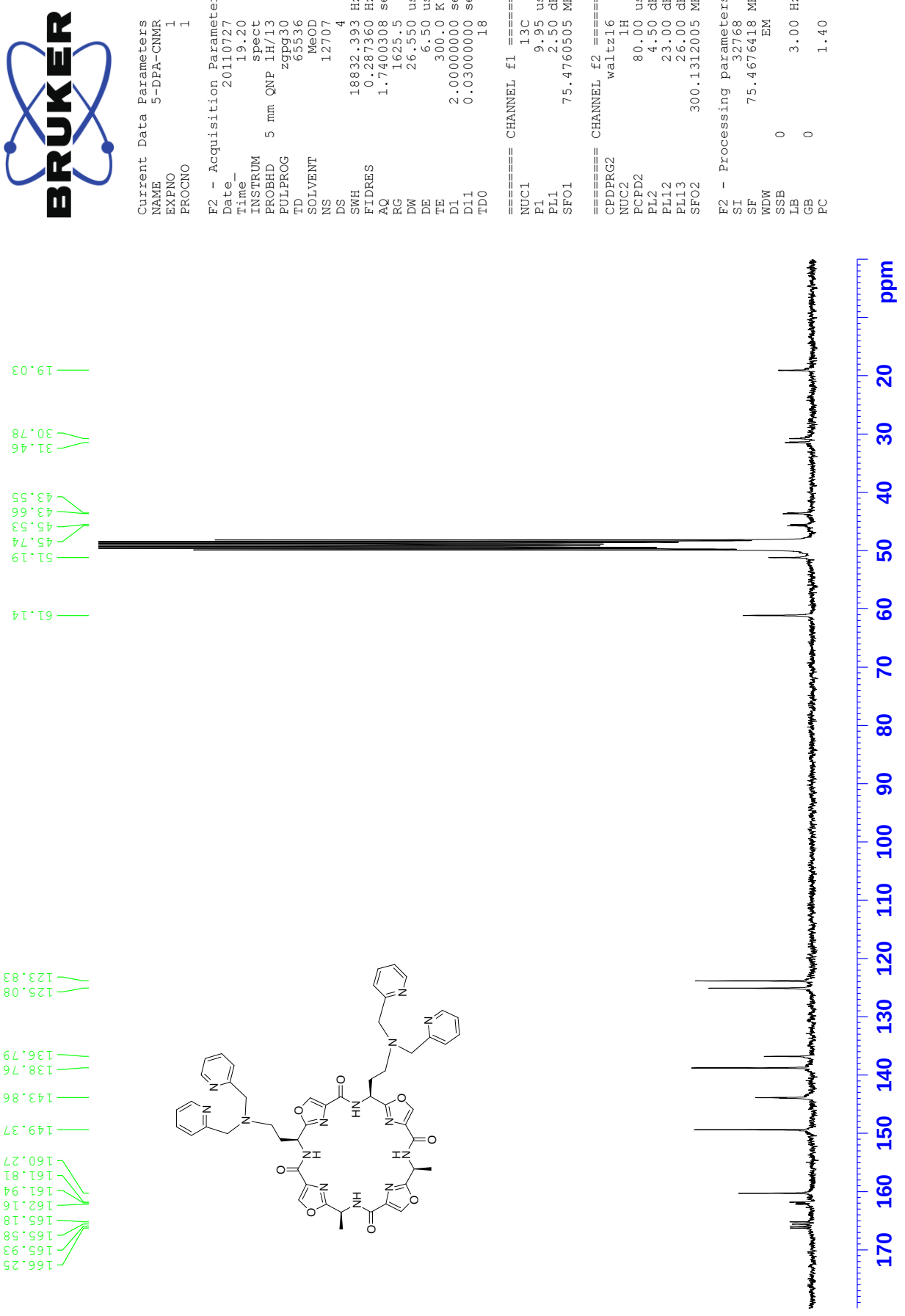
Current Data Parameters
NAME 5-DPA-CNMR
EXPNO 1
PROCNO 1
F2 - Acquisition Parameters
Date_ 20110727
Time 19.20
INSTRUM spect
PROBHD 5 mm QNP 1H/13
PULPROG zgpg30
TD 65536
SOLVENT MeOD
NS 12707
DS 4
SWH 18832.393 Hz
FIDRES 0.287360 Hz
AQ 1.7400308 sec
RG 1625.5
DW 26.550 usec
DE 6.50 usec
TE 300.0 K
D1 2.00000000 sec
D11 0.03000000 sec
TD0 18
======== CHANNEL f1 ========
NUC1 13C
P1 9.95 usec
PL1 2.50 dB
SFO1 75.4760505 MHz
======== CHANNEL f2 ========
CPDPRG2 waltz16
NUC2 1H
PCPD2 80.00 usec
PL2 4.50 dB
PL12 23.00 dB
PL13 26.00 dB
SFO2 300.1312005 MHz
F2 - Processing parameters
SI 32768
SF 75.4676418 MHz
WDW EM
SSB 0
LB 3.00 Hz
GB 0
PC 1.40
19.03
30.78
31.46
43.55
43.66
45.53
45.74
51.19
61.14
123.83
125.08
136.79
138.76
143.86
149.37
160.27
161.81
161.94
162.16
165.18
165.58
165.93
166.25
ppm
170
160
150
140
130
120
110
100
90
80
70
60
50
40
30
20

^{1}H and ^{13}C NMR spectra of compound 6

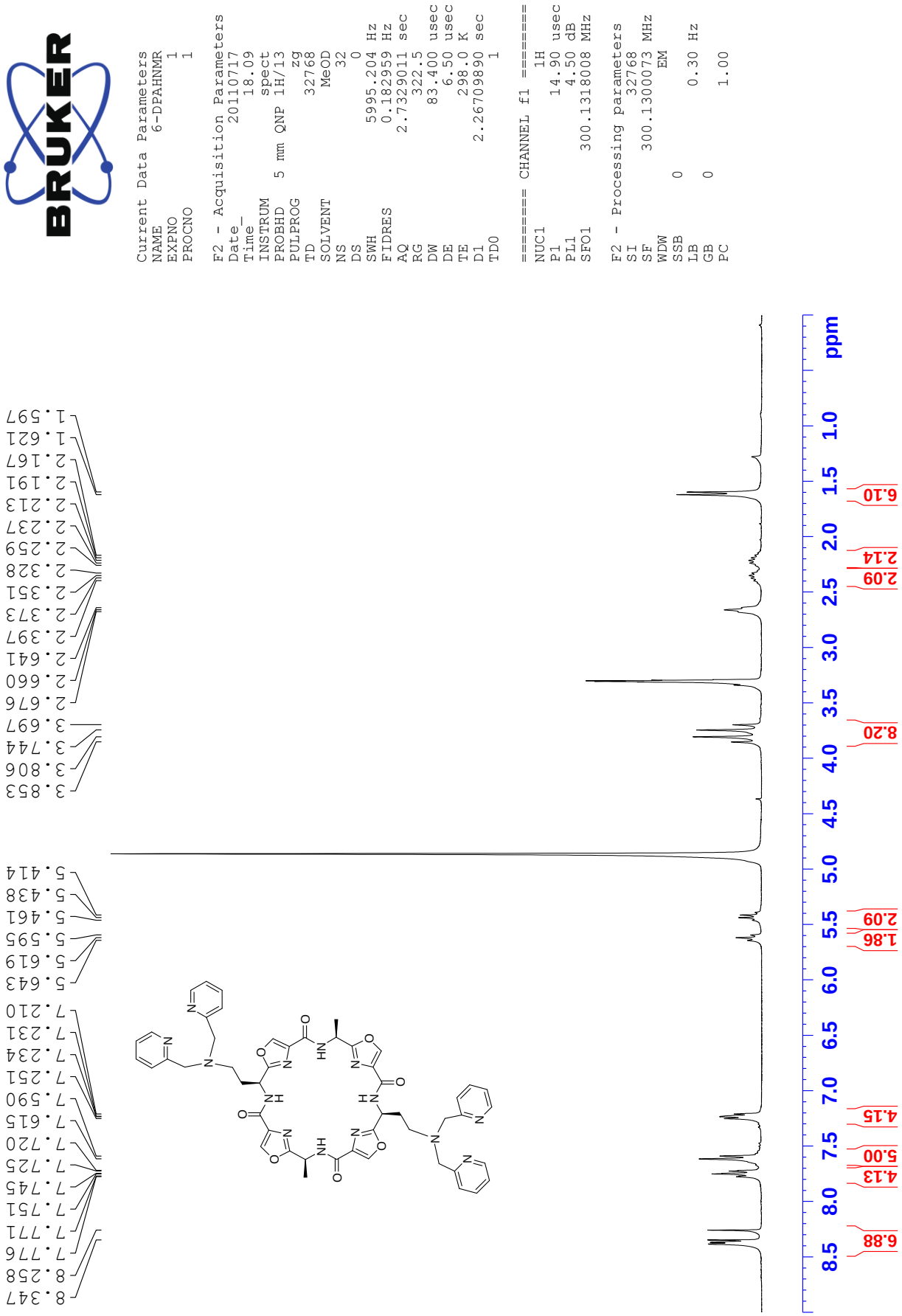

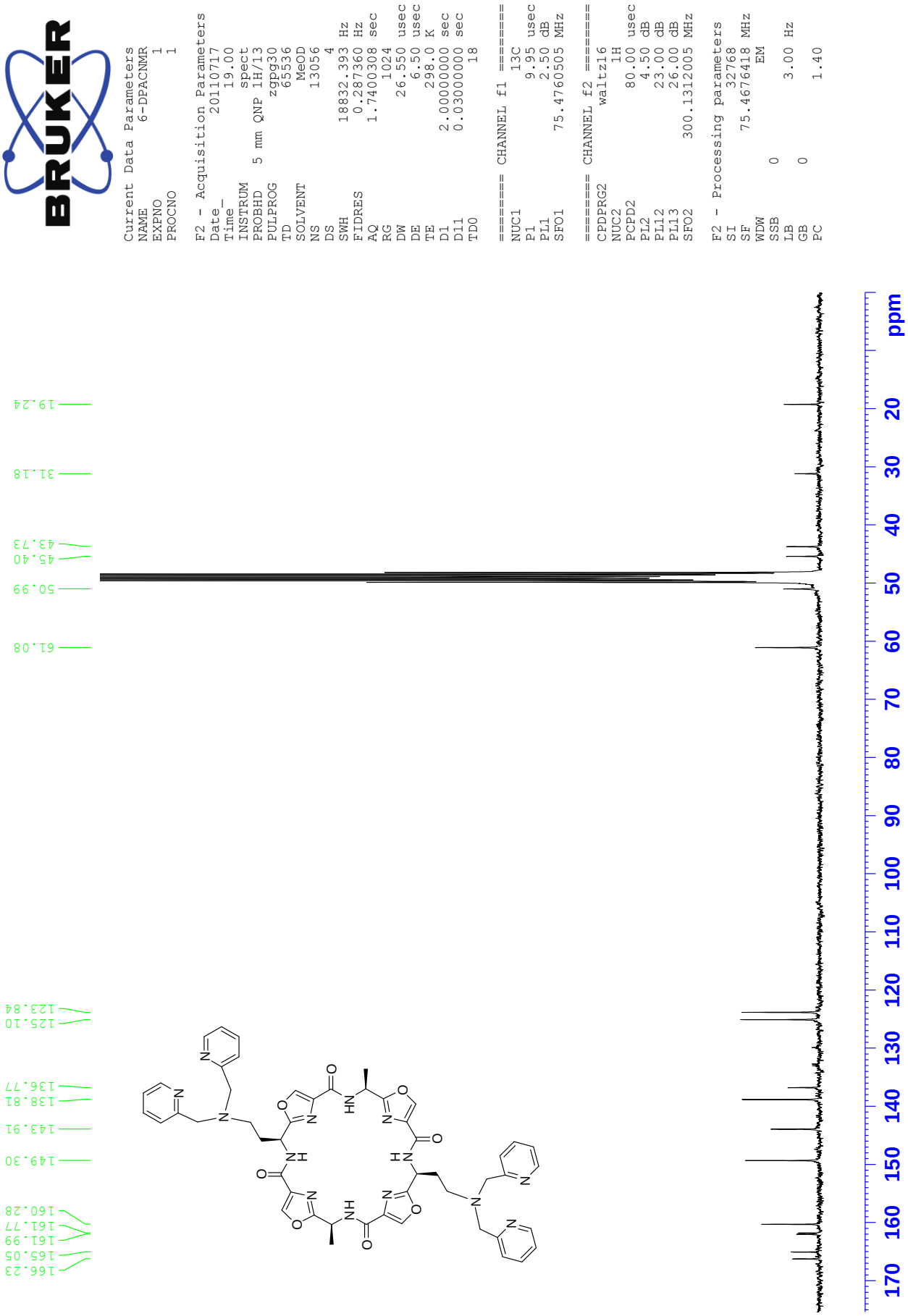
Current Data Parameters
NAME 6-DPACNMR
EXPNO 1
PROCNO 1
F2 - Acquisition Parameters
Date_ 20110717
Time_ 19.00
INSTRUM spect
PROBHD 5 mm QNP 1H/13
PULPROG zgpg30
TD 65536
SOLVENT MeOD
NS 13056
DS 4
SWH 18832.393 Hz
FIDRES 0.287360 Hz
AQ 1.7400308 sec
RG 1024
DW 26.550 usec
DE 6.50 usec
TE 298.0 K
D1 2.00000000 sec
D11 0.03000000 sec
TD0 18
======== CHANNEL f1 ========
NUC1 13C
P1 9.95 usec
PL1 2.50 dB
SFO1 75.4760505 MHz
======== CHANNEL f2 ========
CPDPRG2 waltz16
NUC2 1H
PCPD2 80.00 usec
PL2 4.50 dB
PL12 23.00 dB
PL13 26.00 dB
SFO2 300.1312005 MHz
F2 - Processing parameters
SI 32768
SF 75.4676418 MHz
WDW EM
SSB 0
LB 3.00 Hz
GB 0
PC 1.40
19.24
31.18
43.73
45.40
50.99
61.08
123.84
125.10
136.77
138.81
143.91
149.30
160.28
161.77
161.99
165.05
166.23
ppm
20
30
40
50
60
70
80
90
100
110
120
130
140
150
160
170

^{1}H and ^{13}C NMR spectra of compound 7

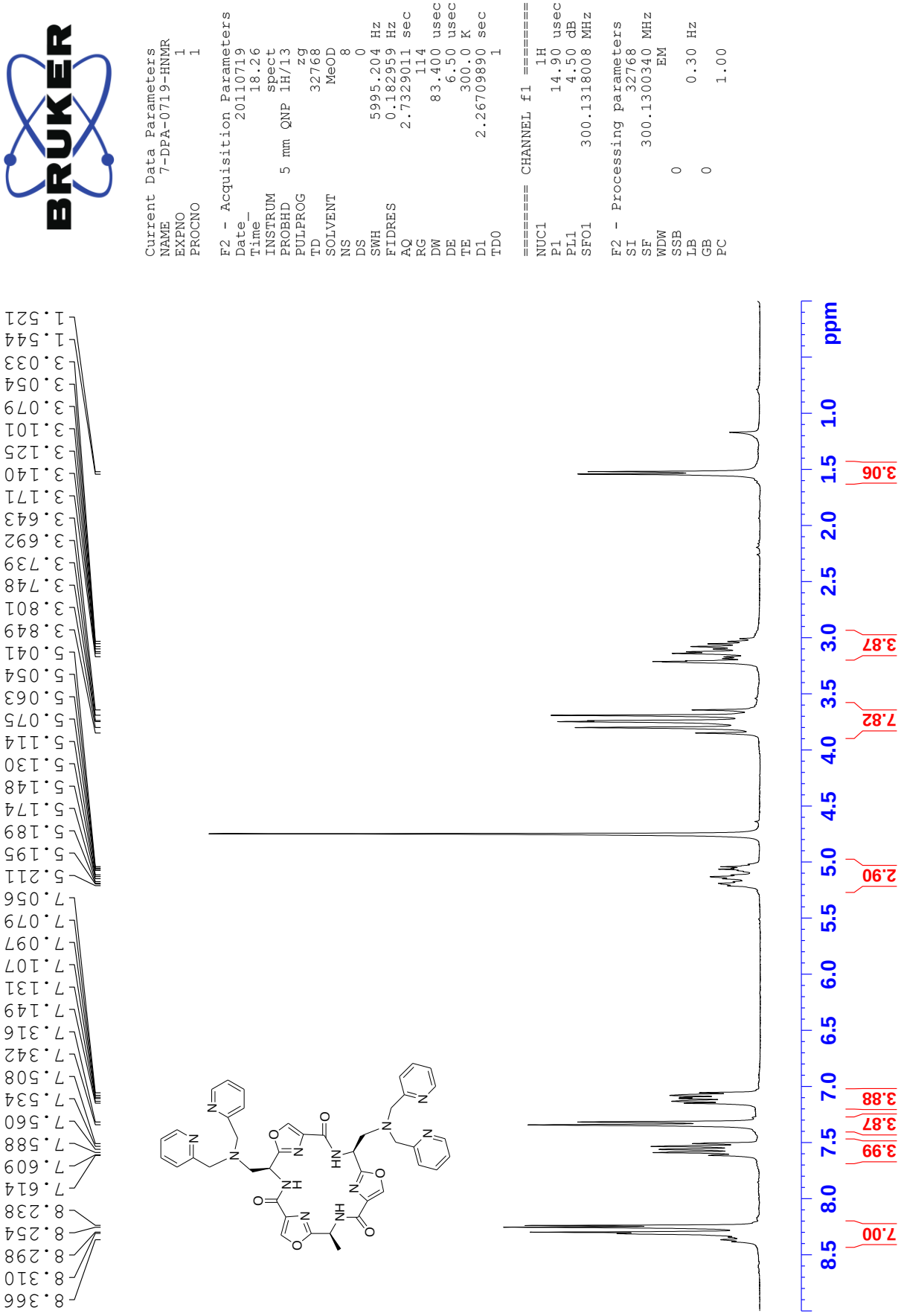

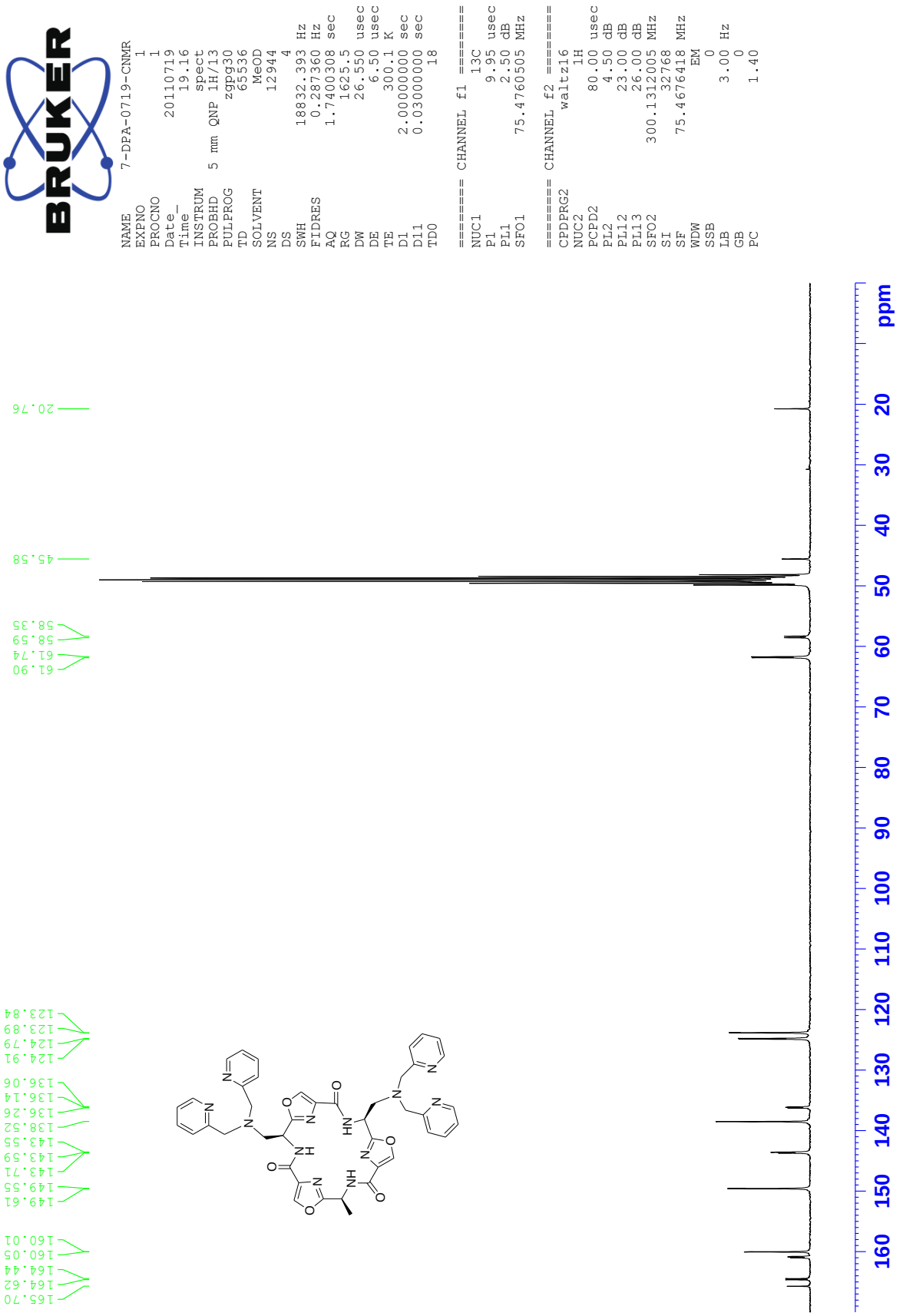

^{1}HNMR spectra of compound 8

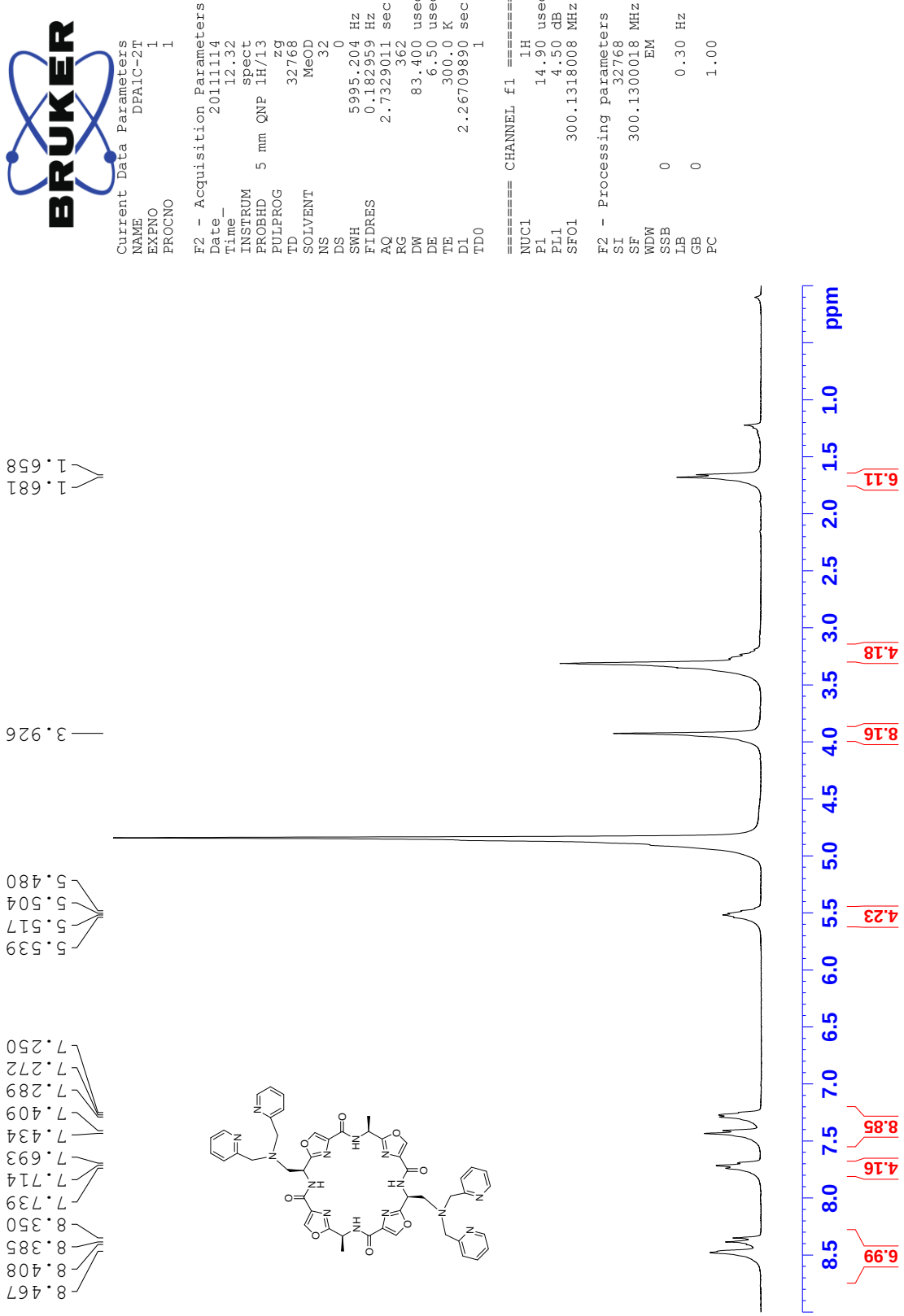

2. General procedures for anion binding studies

UV-Vis data was recorded using a Varian Cary 4000 UV-Vis Spectrophotometer. Temperature control was provided by a Varian Cary PCB 150 Water Peltier System. pH values were determined using an Mettler Toledo SevenEasy pH meter.

Anion Binding Studies under Mimicked Physiological Conditions

All titrations were performed in aqueous solutions buffered at pH 7.4 with HEPES (5 mM) in the presence of 145 mM sodium chloride, at 25 °C.

Anion Binding Studies in Physiological Saline Solution

All titrations were performed in a modified Krebs buffer solution, with a pH adjusted to 7.4 with hydrochloric acid, at 25 °C. Krebs buffer solution comprises of NaCl (137 mM), KCl (5.4 mM), $CaCl_2$ (2.8 mM), $MgSO_4$ (1.2 mM), KH_2PO_4 (0.4 mM), NaH_2PO_4 (0.3 mM), glucose (10 mM) and Tris-base (10 mM).

2.1 General procedure for titrating indicators with receptors 1–9·Zn_2

Stock solutions of each indicator **PV** or **PR** (20 μM) or **BPR** (10 μM), and of each receptor (1000 μM) were prepared. To a 1 cm quartz glass cuvette was added a solution of the indicator (2.5 mL) and to another matched quartz glass cuvette was added the buffer solution as the blank (2.5 mL). The absorbance was recorded from 250 nm to 750 nm. Aliquots of a solution containing the receptor were then added to both the sample and the blank cuvettes. After each addition, the resulting solution was stirred for at least 30 seconds and the absorbance was recorded. Typically, up to 10 equivalents of the receptor were added to the solution.

To determine association constants for the receptor-indicator complexes, global analysis of the absorbance data over the range 300-720 nm was carried out using a nonlinear least-squares curve fitting procedure, based on the equilibria described for 1:1 binding (for PV) or stepwise 1:1 and 2:1 binding (for BPR), using the commercially available software program HypSpec® (Hyperquad® package).[4]

2.2 General procedure for titrating receptor-indicator ensembles with anions

A stock solution of a 1:1 receptor-indicator ensemble was prepared by mixing equimolar amounts of each indicator (20 μM) and the receptor (20 μM) (in case of **BPR**, 10 μM each). Stock solutions of the anion (2000 μM) were prepared using the appropriate sodium salt. To a 1 cm quartz glass cuvette was added a solution of the receptor-indicator ensemble (2.5 mL) and to another matched quartz glass cuvette was added a solution of the same concentration of the receptor as the blank (2.5 mL). The absorbance was recorded from 250 nm to 750 nm. Aliquots of a solution containing the anion were then added to both the sample and the blank cuvettes. After each addition, the resulting solution was stirred for at least 30 seconds and the absorbance was recorded. Typically, up to 10 equivalents of the anion were added to the solution.

To determine association constants for the receptor-anion complexes, global analysis of the absorbance data over the range 300-720 nm was carried out using a nonlinear least-squares curve fitting procedure, based on the equilibria described for indicator displacement,[5] using the commercially available software program HypSpec® (Hyperquad® package).[4]

3. Anion binding studies conducted in HEPES buffer solution

3.1 Titrating indicators with complexes 1–9•Zn_2 in HEPES buffer solution.

Measurement conditions: aqueous solution of HEPES buffer (5 mM, 145 mM NaCl, pH 7.4) at 25 °C.

3.1.1 Receptor 1•Zn_2

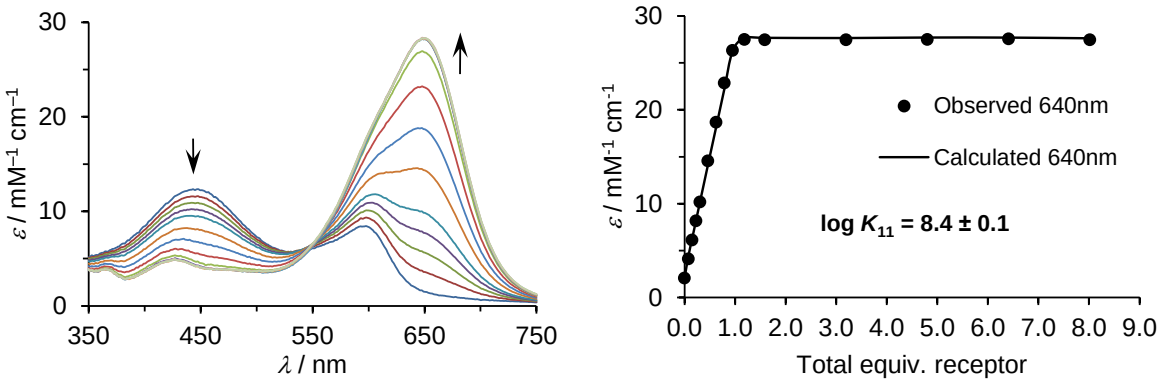

Figure S1. Left: Absorbance changes for PV solution (20 μM) upon addition of 1•Zn_2 (0-10 equiv.). Right: 1:1 fitting curve at 640 nm.

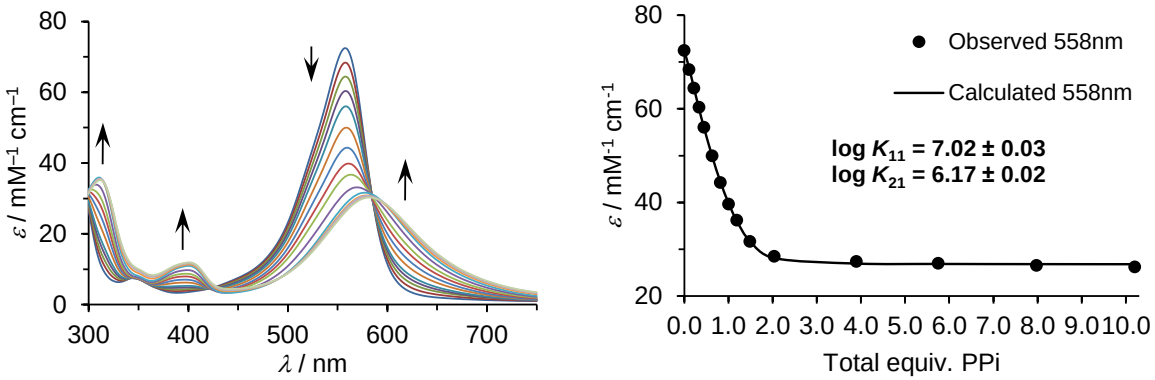

Figure S2. Left: Absorbance changes for BPR solution (10 μM) upon addition of 1•Zn_2 (0-10 equiv.). Right: fitting curve to a stepwise 1:1 and 2:1 at 558 nm.

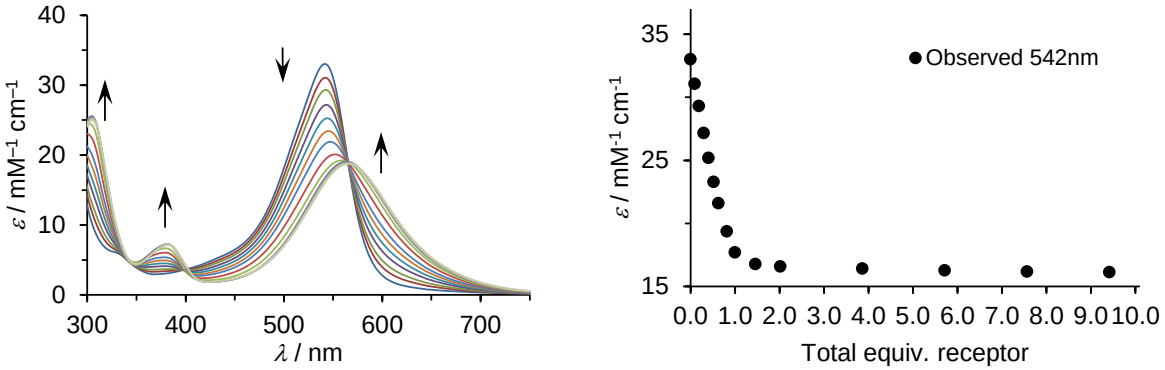

Figure S3. Left: Absorbance changes for PR solution (20 μM) upon addition of 1•Zn_2 (0-10 equiv.). Right: Absorbance at 542 nm, a satisfactory fitting curve was not obtained.

3.1.2 Receptor 2•Zn_2

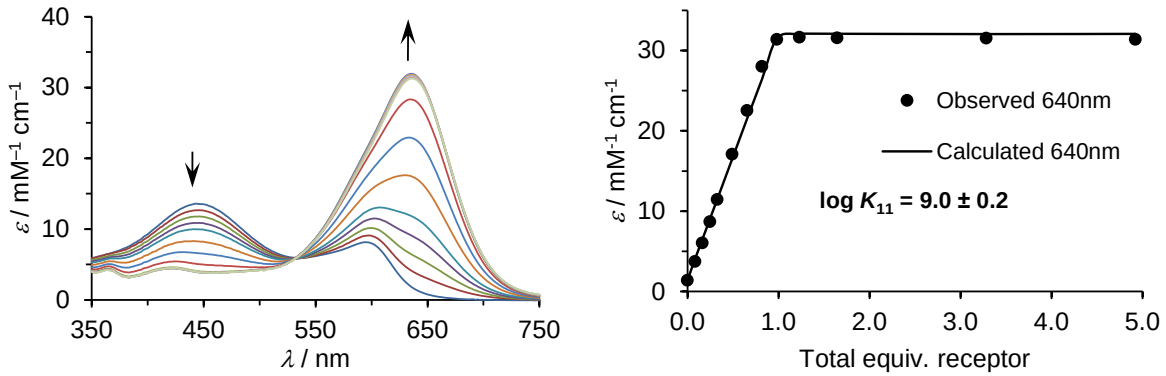

Figure S4. Left: Absorbance changes for PV solution (20 μM) upon addition of 2•Zn_2 (0-10 equiv.). Right: 1:1 fitting curve at 640 nm.

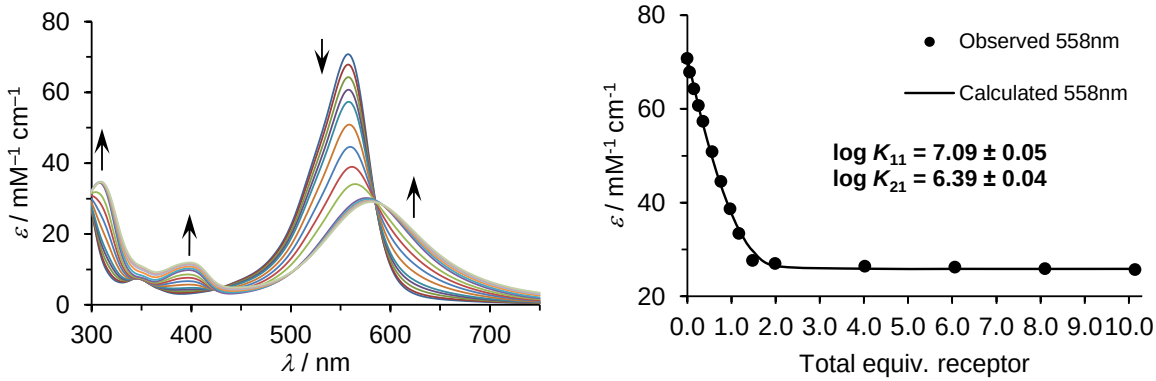

Figure S5. Left: Absorbance changes for BPR solution (10 μM) upon addition of 2•Zn_2 (0-10 equiv.). Right: fitting curve to a stepwise 1:1 and 2:1 at 558 nm.

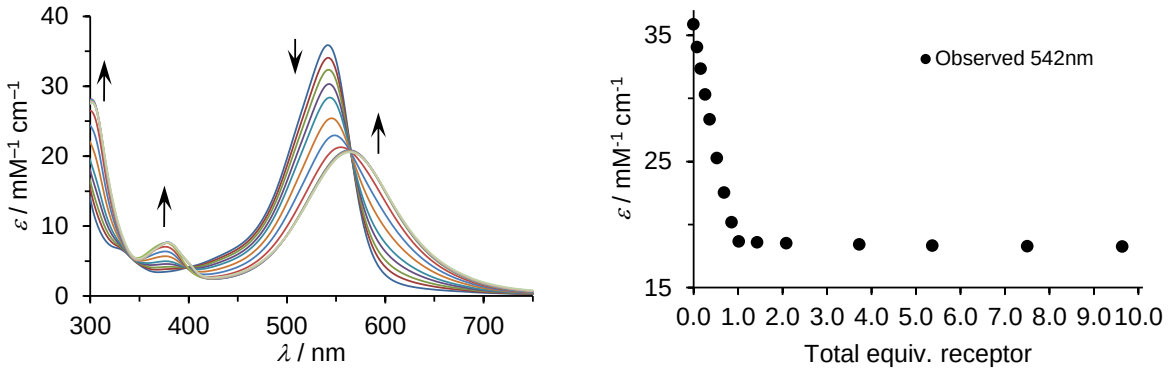

Figure S6. Left: Absorbance changes for PR solution (20 μM) upon addition of 2•Zn_2 (0-10 equiv.). Right: Absorbance at 542 nm, a satisfactory fitting curve was not obtained.

3.1.3 Receptor 3•Zn_2

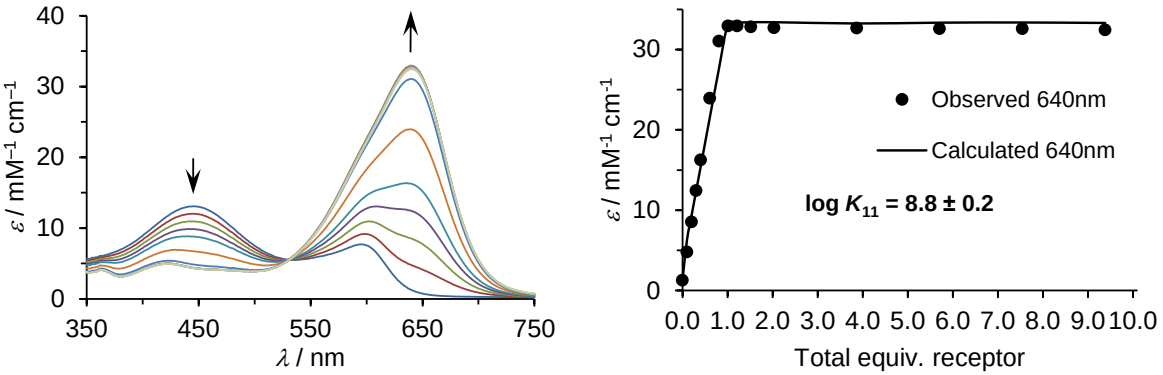

Figure S7. Left: Absorbance changes for PV solution (20 μM) upon addition of 3•Zn_2 (0-10 equiv.). Right: 1:1 fitting curve at 640 nm.

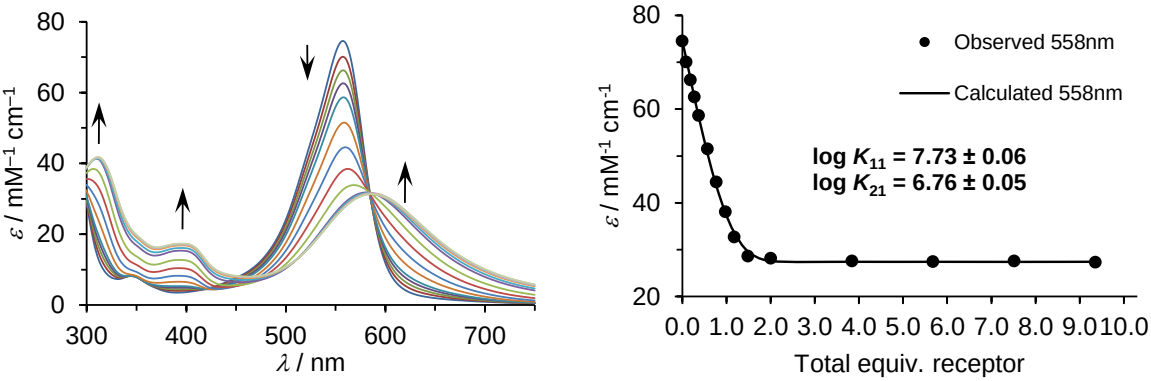

Figure S8. Left: Absorbance changes for BPR solution (10 μM) upon addition of 3•Zn_2 (0-10 equiv.). Right: fitting curve to a stepwise 1:1 and 2:1 at 558 nm.

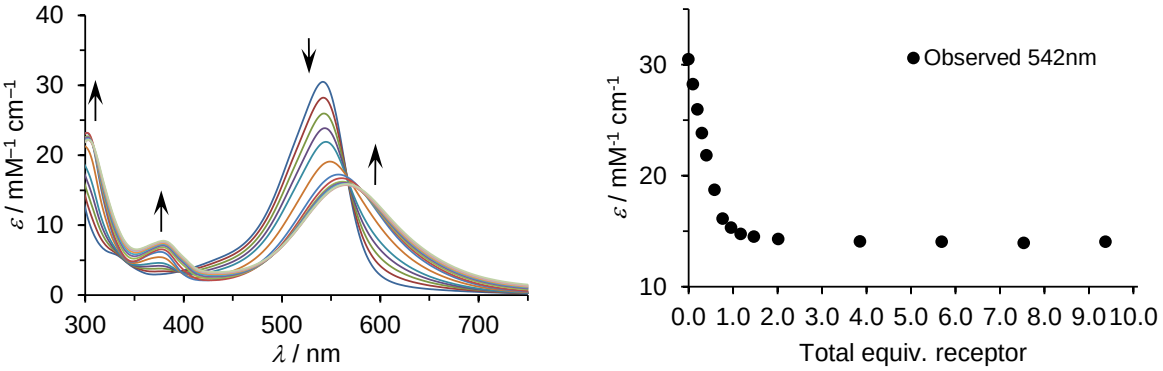

Figure S9. Left: Absorbance changes for PR solution (20 μM) upon addition of 3•Zn_2 (0-10 equiv.). Right: Absorbance at 542 nm, a satisfactory fitting curve was not obtained.

3.1.4 Receptor 4•Zn_2

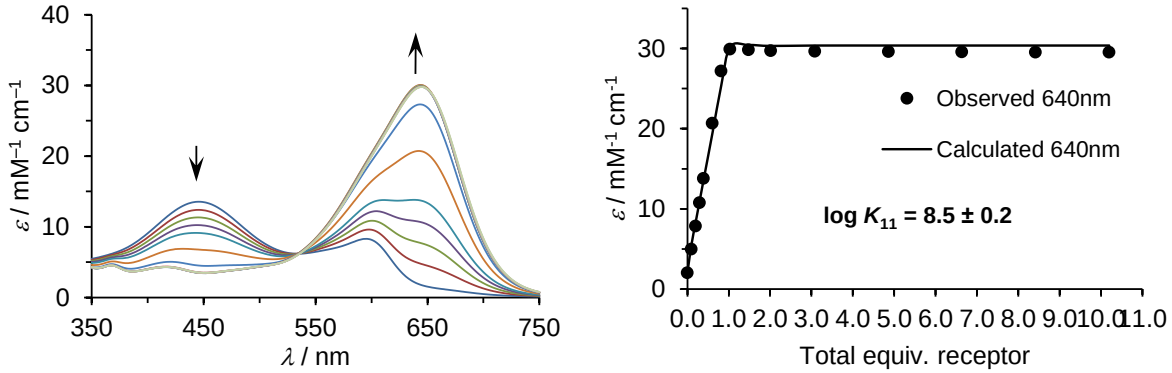

Figure S10. Left: Absorbance changes for PV solution (20 μM) upon addition of 4•Zn_2 (0-10 equiv.). Right: 1:1 fitting curve at 640 nm.

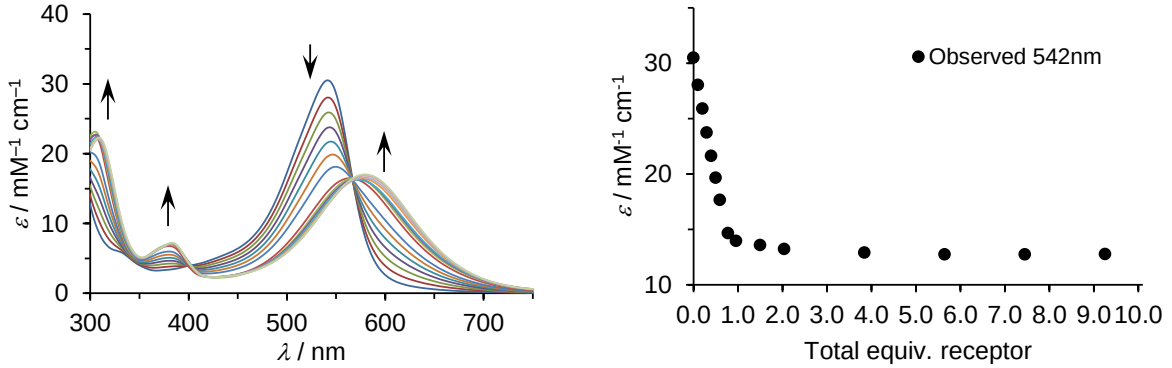

Figure S11. Left: Absorbance changes for PR solution (20 μM) upon addition of 4•Zn_2 (0-10 equiv.). Right: Absorbance at 542 nm, a satisfactory fitting curve was not obtained.

3.1.5 Receptor 5•Zn_2

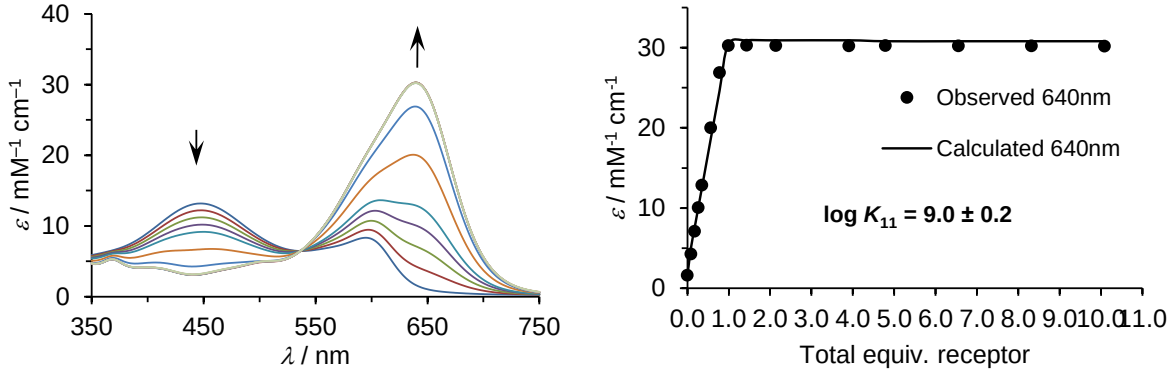

Figure S12. Left: Absorbance changes for PV solution (20 μM) upon addition of 5•Zn_2 (0-10 equiv.). Right: 1:1 fitting curve at 640 nm.

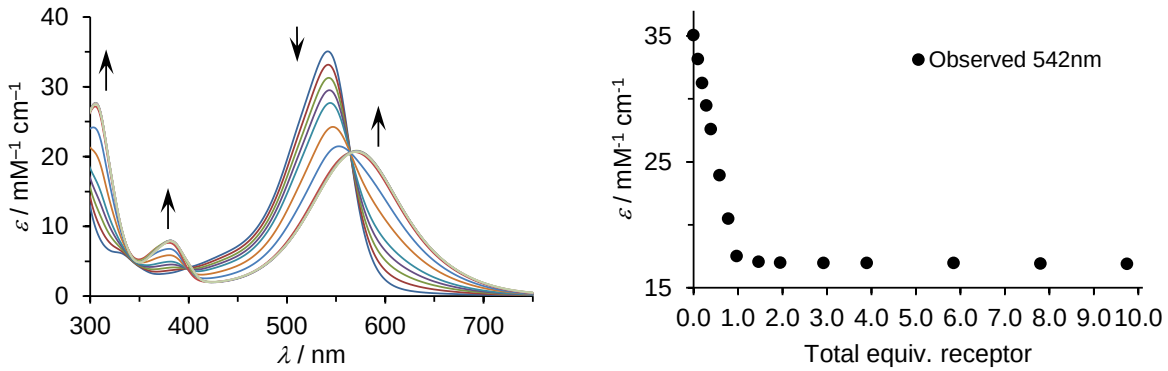

Figure S13. Left: Absorbance changes for PR solution (20 μM) upon addition of 5•Zn_2 (0-10 equiv.). Right: Absorbance at 542 nm, a satisfactory fitting curve was not obtained.

3.1.6 Receptor 6•Zn_2

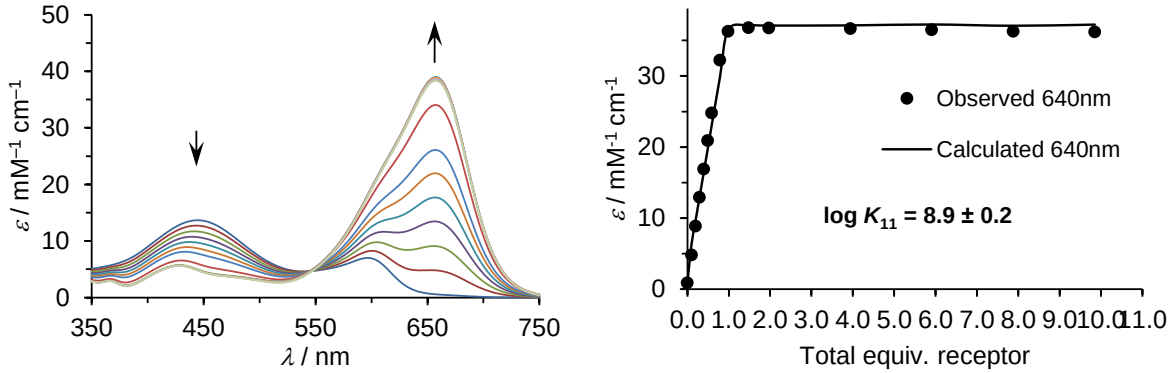

Figure S14. Left: Absorbance changes for PV solution (20 μM) upon addition of 6•Zn_2 (0-10 equiv.). Right: 1:1 fitting curve at 640 nm.

3.1.7 Receptor 7•Zn_2

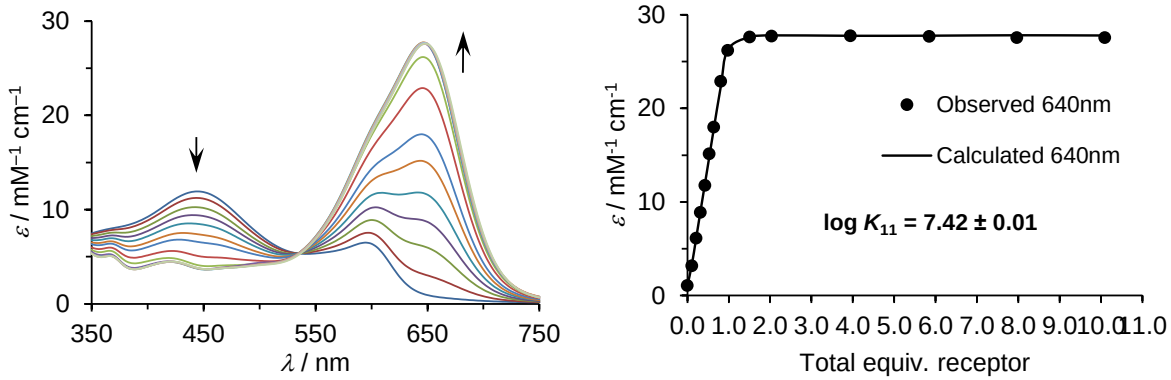

Figure S15. Left: Absorbance changes for PV solution (20 μM) upon addition of 7•Zn_2 (0-10 equiv.). Right: 1:1 fitting curve at 640 nm.

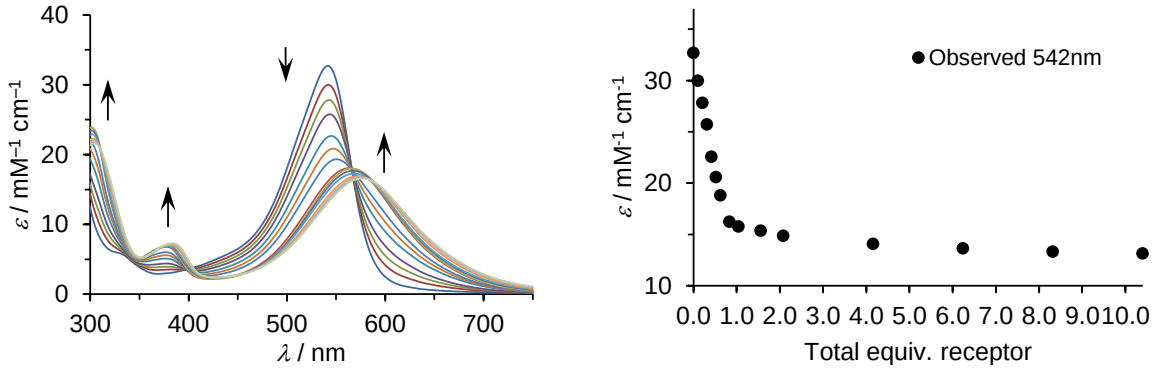

Figure S16. Left: Absorbance changes for PR solution (20 μM) upon addition of 7•Zn_2 (0-10 equiv.). Right: Absorbance at 542 nm, a satisfactory fitting curve was not obtained.

3.1.8 Receptor 8•Zn_2

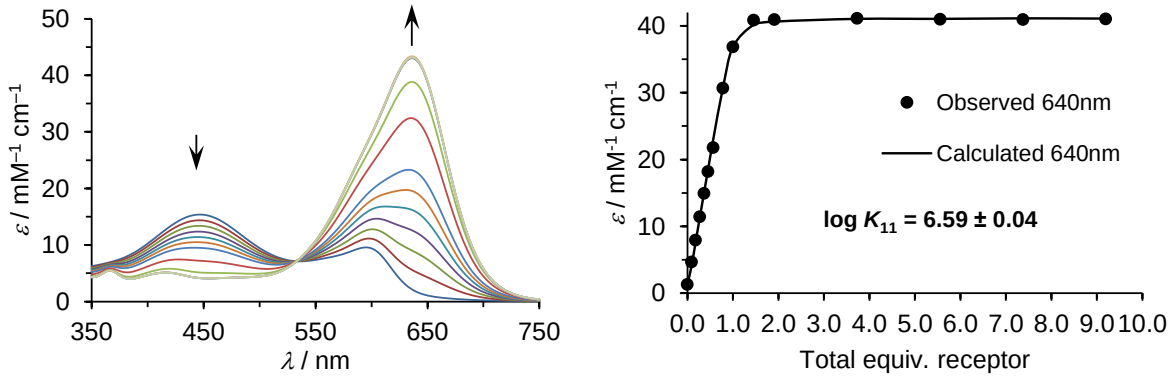

Figure S17. Left: Absorbance changes for PV solution (20 μM) upon addition of 8•Zn_2 (0-10 equiv.). Right: 1:1 fitting curve at 640 nm.

3.1.9 Receptor 9•Zn_2

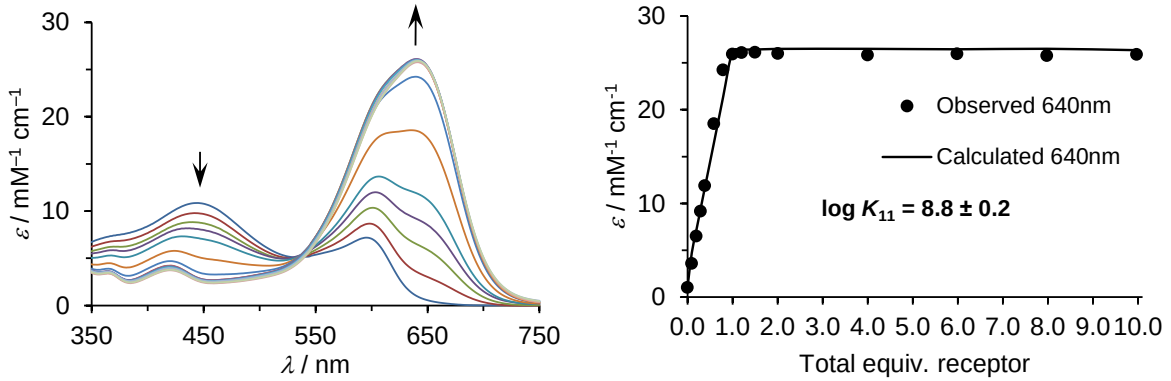

Figure S18. Left: Absorbance changes for PV solution (20 μM) upon addition of 9•Zn_2 (0-10 equiv.). Right: 1:1 fitting curve at 640 nm.

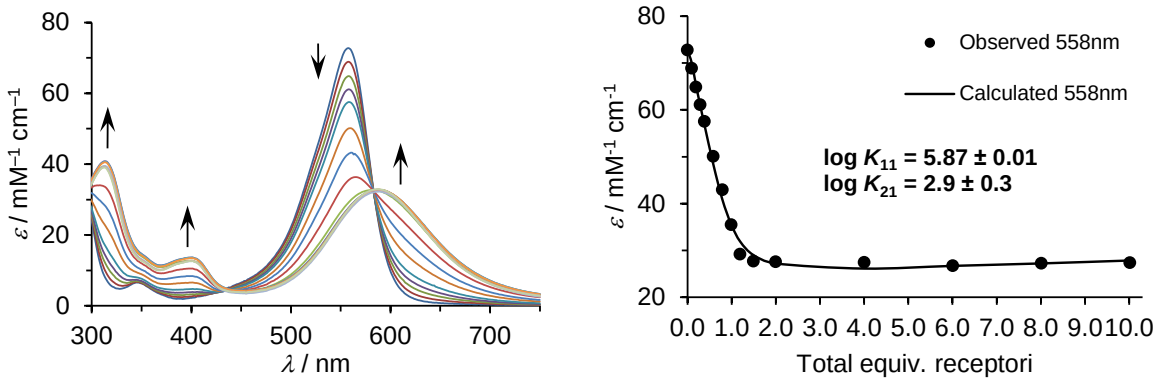

Figure S19. Left: Absorbance changes for BPR solution (10 μM) upon addition of 9•Zn_2 (0-10 equiv.). Right: fitting curve to a stepwise 1:1 and 2:1 at 558 nm.

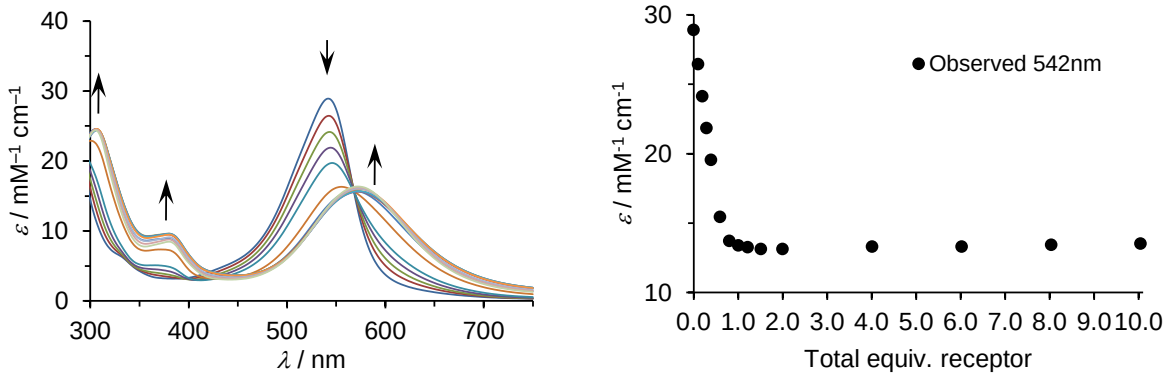

Figure S20. Left: Absorbance changes for PR solution (20 μM) upon addition of 9•Zn_2 (0-10 equiv.). Right: Absorbance at 542 nm, a satisfactory fitting curve was not obtained.

3.2 Job Plots for the receptor-indicator binding of 1–9•Zn_2 and indicators

Measurement conditions: A total concentration of 20 μM was used in aqueous solution of HEPES buffer (5 mM, 145 mM NaCl, pH 7.4), 25 °C.

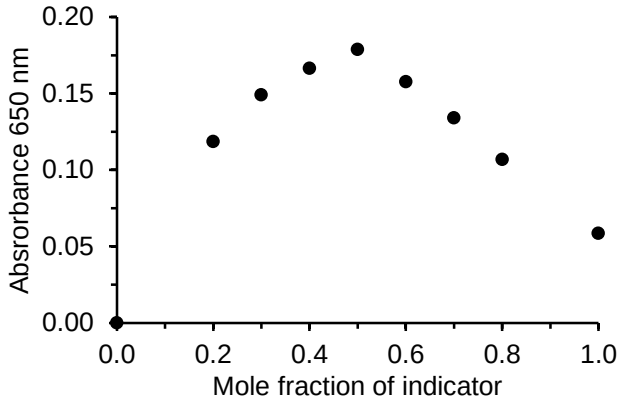

Figure S21. Job's plot for receptor 1•Zn_2 with PV.

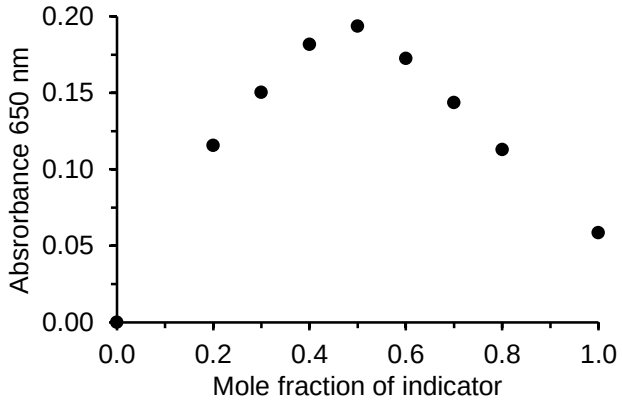

Figure S22. Job's plot for receptor 2•Zn_2 with PV.

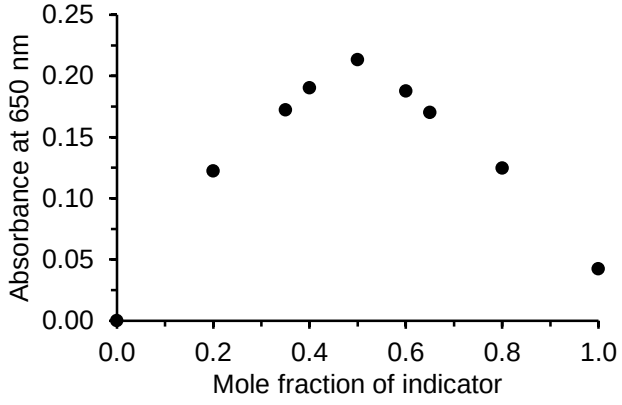

Figure S23. Job's plot for receptor 3•Zn_2 with PV.

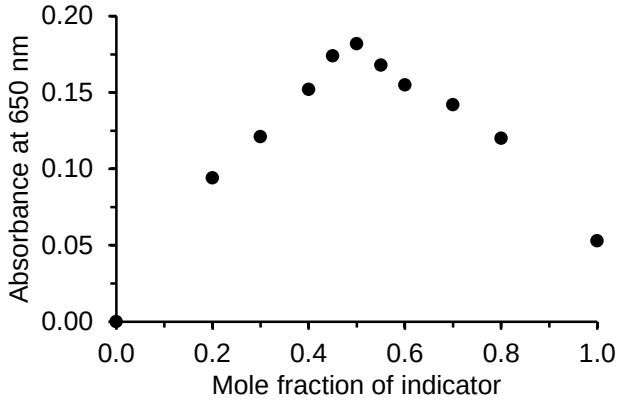

Figure S24. Job's plot for receptor 4•Zn_2 with PV.

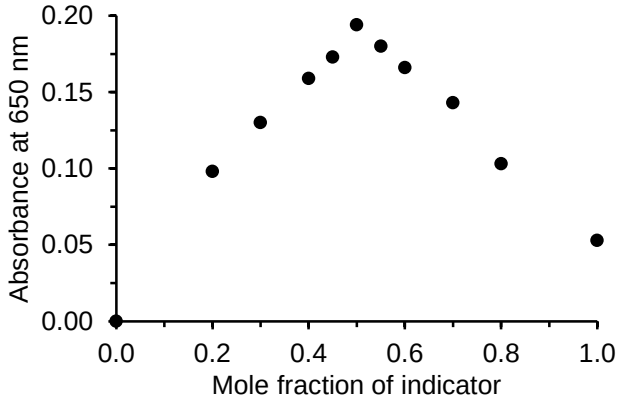

Figure S25. Job's plot for receptor 5•Zn_2 with PV.

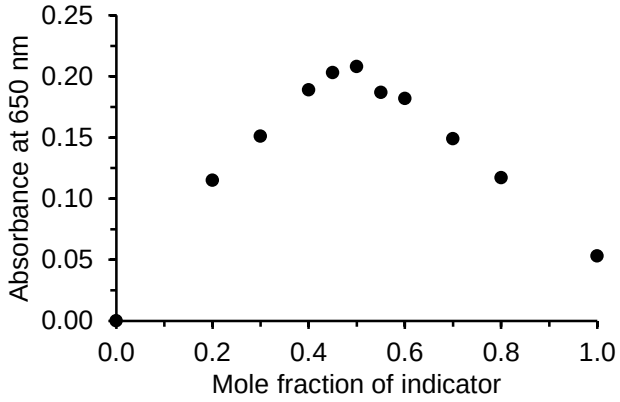

Figure S26. Job's plot for receptor 6•Zn_2 with PV

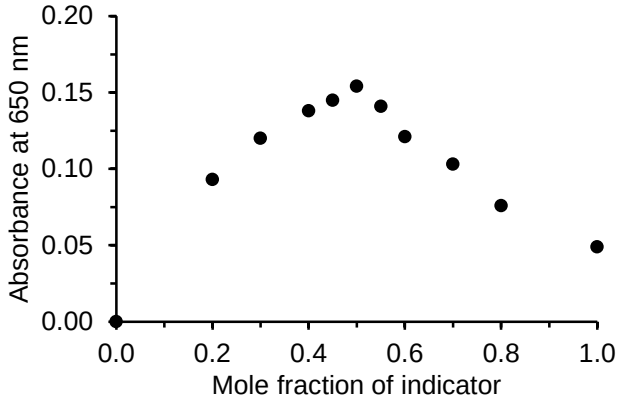

Figure S27. Job's plot for receptor 7•Zn_2 with PV

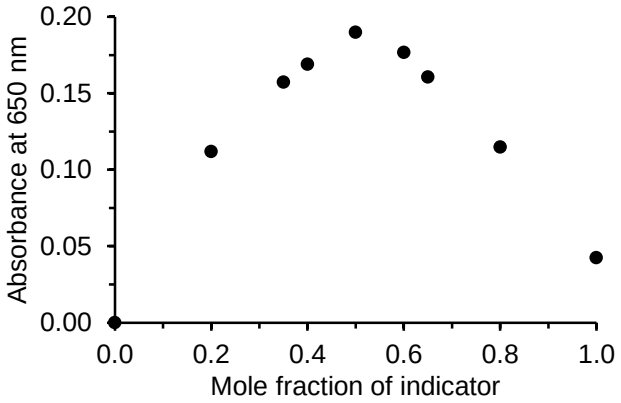

Figure S28. Job's plot for receptor 9•Zn_2 with PV.

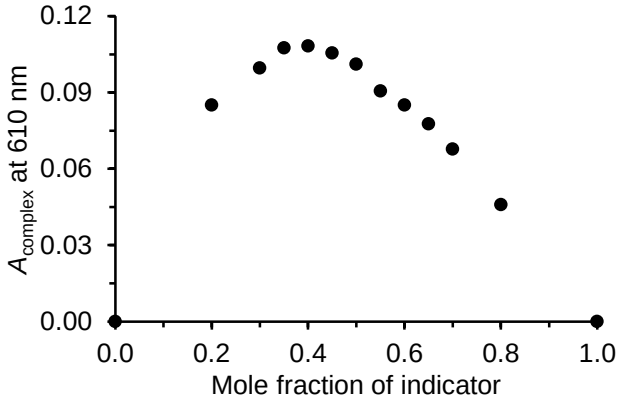

Figure S29. Job's plot for receptor 1•Zn_2 with BPR.

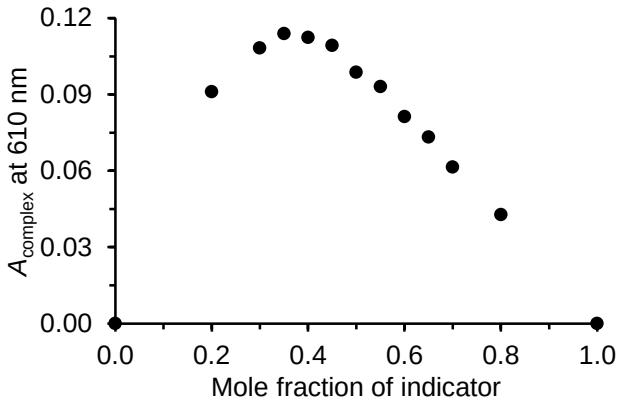

Figure S30. Job's plot for receptor 2•Zn_2 with BPR.

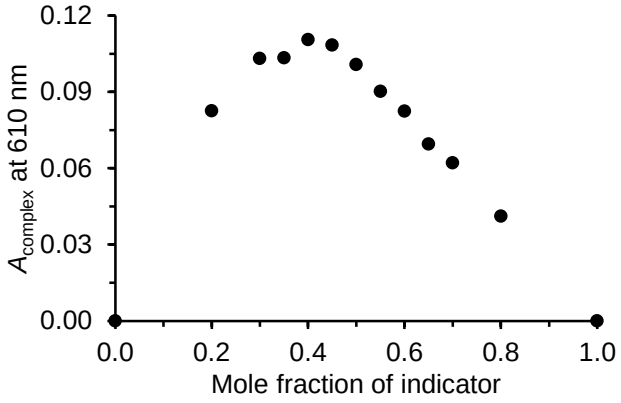

Figure S31. Job's plot for receptor 3•Zn_2 with BPR.

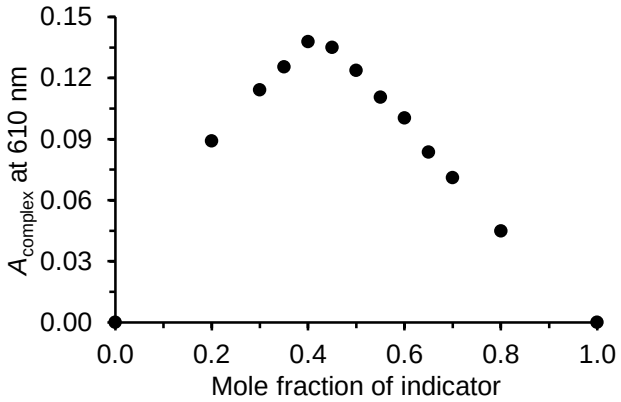

Figure S32. Job's plot for receptor 9•Zn_2 with BPR.

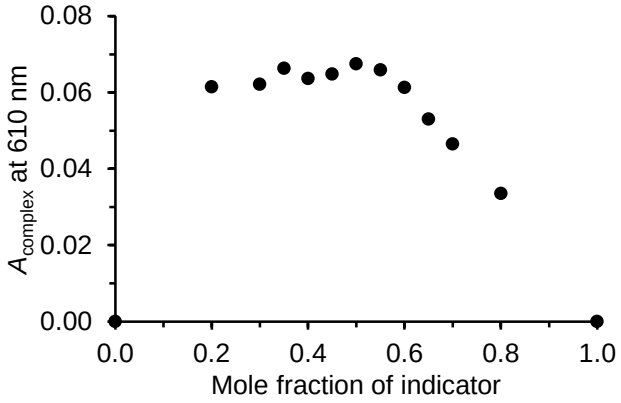

Figure S33. Job's plot for receptor 1•Zn_2 with PR.

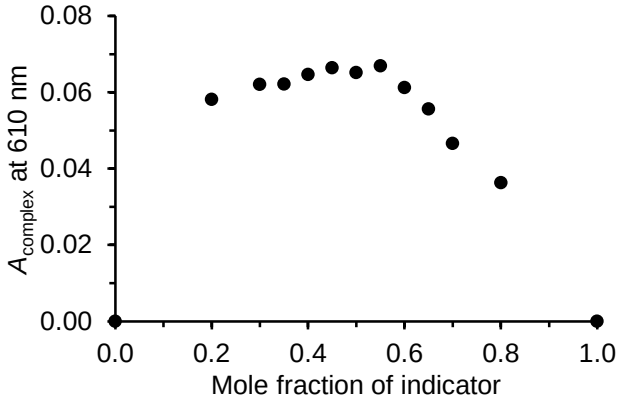

Figure S34. Job's plot for receptor 2•Zn_2 with PR.

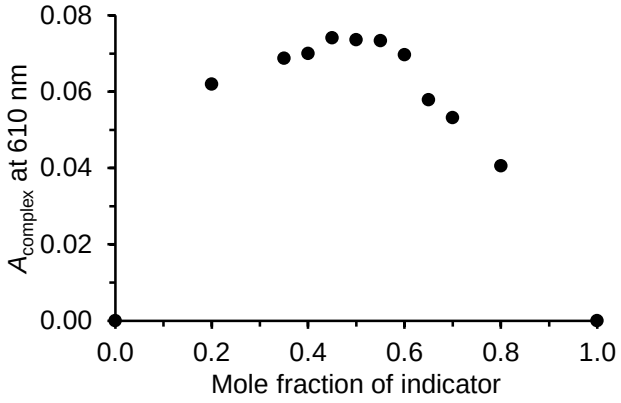

Figure S35. Job's plot for receptor 3•Zn_2 with PR.

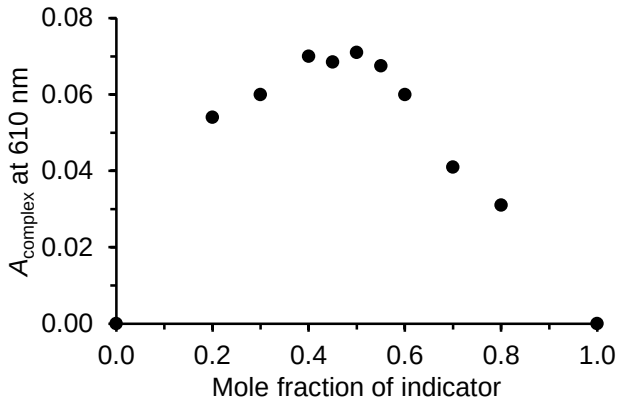

Figure S36. Job's plot for receptor 4•Zn_2 with PR.

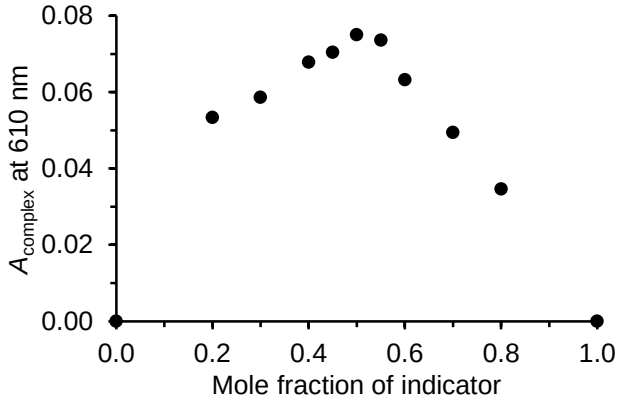

Figure S37. Job's plot for receptor 5•Zn_2 with PR.

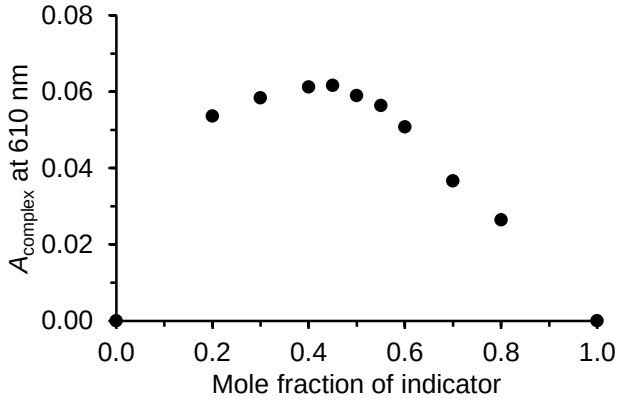

Figure S38. Job's plot for receptor 7•Zn_2 with PR.

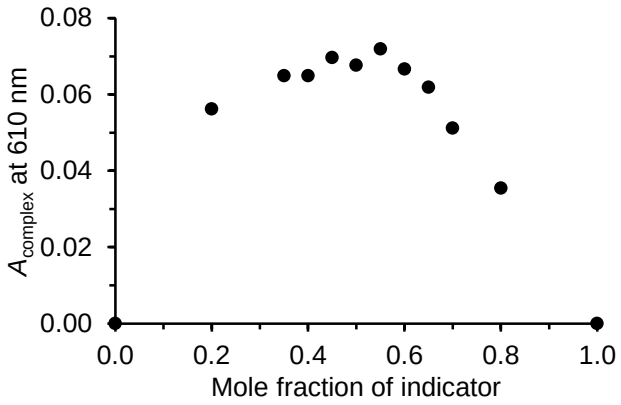

Figure S39. Job's plot for receptor 9•Zn_2 with PR.

3.3 Titrating receptor-indicator ensembles with various anions in saline HEPES buffer solution.

Measurement conditions: aqueous solution of HEPES buffer (5 mM, 145 mM NaCl, pH 7.4) at 25 °C. Anions are added as sodium salts.

3.3.1 Receptor 1•Zn_2

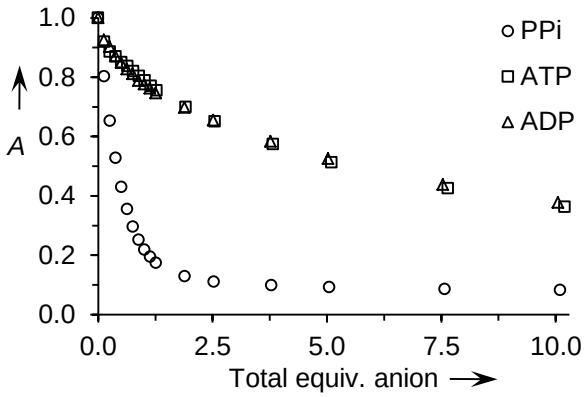

Figure S40. Absorbance changes at 640 nm for 1:1 mixture of 1•Zn_2:PV (20 μM) upon addition of anions (0-10 equiv.).

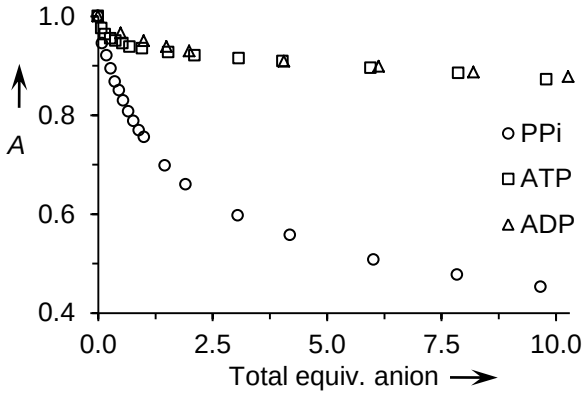

Figure S41. Absorbance changes at 600 nm for 1:1 mixture of 1•Zn_2:PR (20 μM) upon addition of anions (0-10 equiv.).

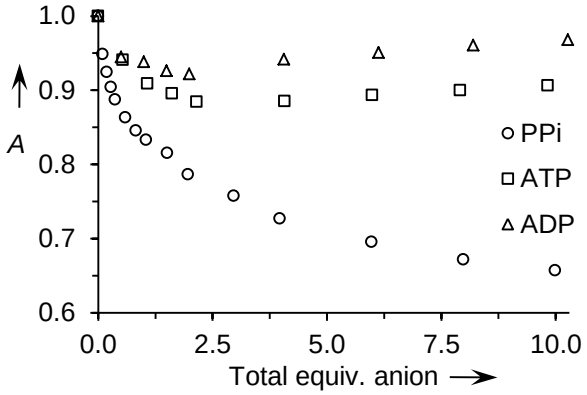

Figure S42. Absorbance changes at 610 nm for 1:1 mixture of 1•Zn_2:BPR (10 μM) upon addition of anions (0-10 equiv.).

3.3.2 Receptor 2•Zn_2

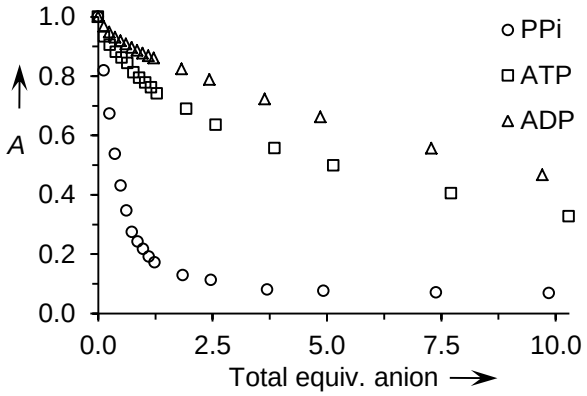

Figure S43. Absorbance changes at 640 nm for 1:1 mixture of 2•Zn_2:PV (20 μM) upon addition of anions (0-10 equiv.).

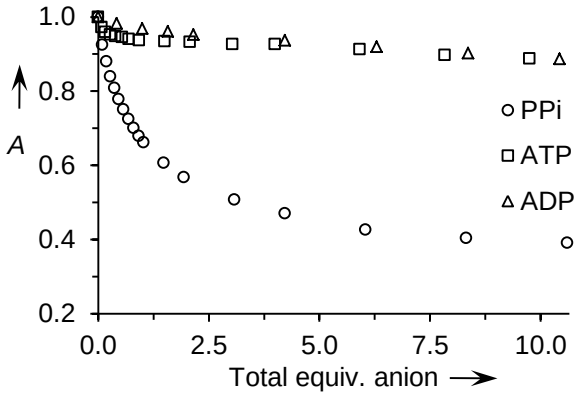

Figure S44. Absorbance changes at 600 nm for 1:1 mixture of 2•Zn_2:PR (20 μM) upon addition of anions (0-10 equiv.).

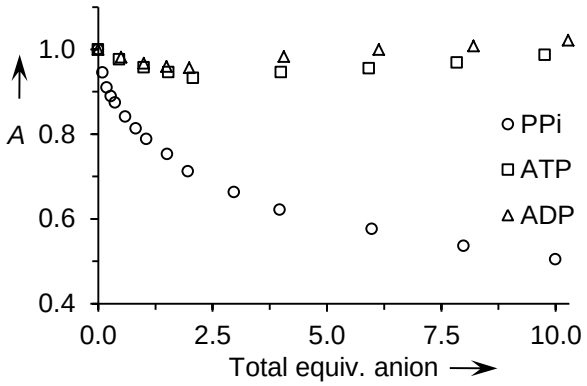

Figure S45. Absorbance changes at 610 nm for 1:1 mixture of 2•Zn_2:BPR (10 μM) upon addition of anions (0-10 equiv.).

3.3.3 Receptor 3•Zn_2

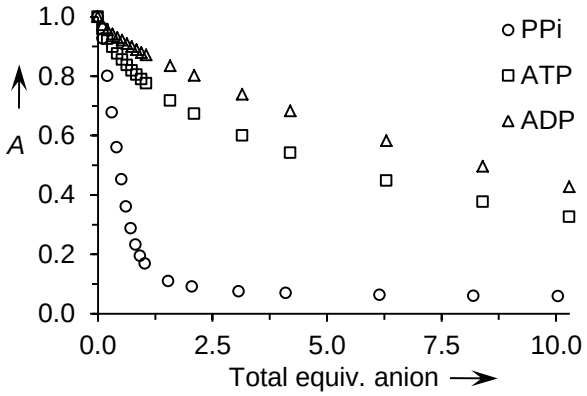

Figure S46. Absorbance changes at 640 nm for 1:1 mixture of 3•Zn_2:PV (20 μM) upon addition of anions (0-10 equiv.).

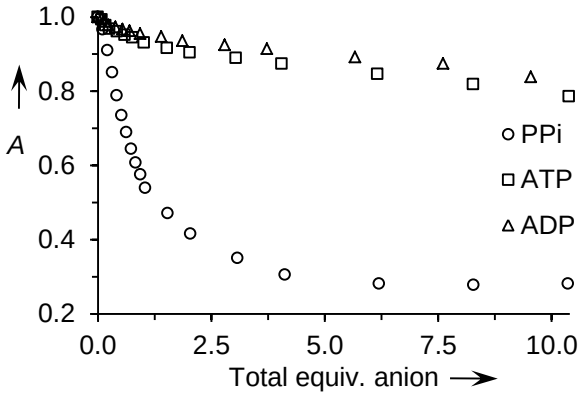

Figure S47. Absorbance changes at 600 nm for 1:1 mixture of 3•Zn_2:PR (20 μM) upon addition of anions (0-10 equiv.).

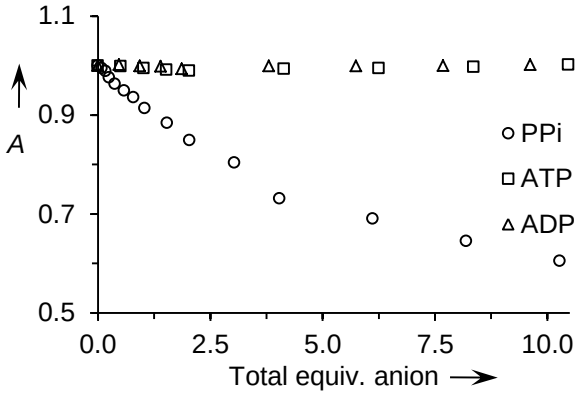

Figure S48. Absorbance changes at 610 nm for 1:1 mixture of 3•Zn_2:BPR (10 μM) upon addition of anions (0-10 equiv.).

3.3.4 Receptor 4•Zn_2

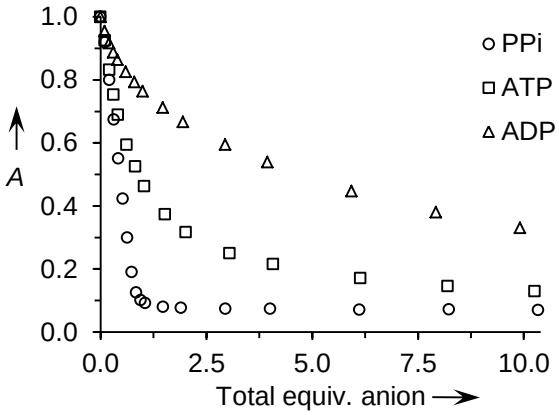

Figure S49. Absorbance changes at 640 nm for 1:1 mixture of 4•Zn_2:PV (20 μM) upon addition of anions (0-10 equiv.).

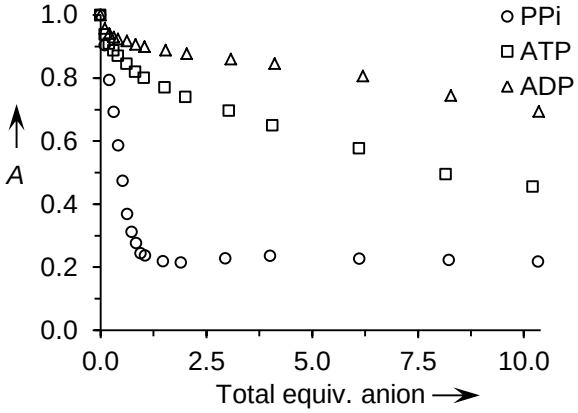

Figure S50. Absorbance changes at 600 nm for 1:1 mixture of 4•Zn_2:PR (20 μM) upon addition of anions (0-10 equiv.).

3.3.5 Receptor 5•Zn_2

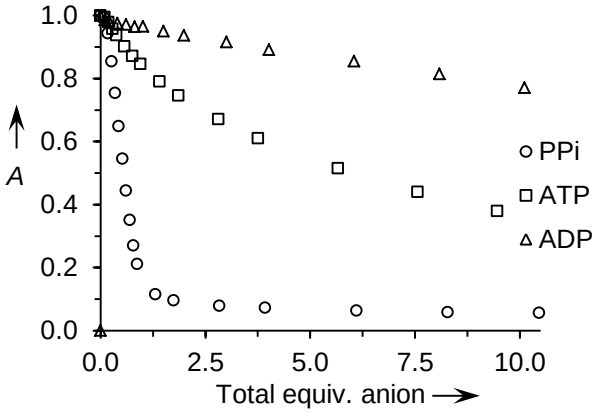

Figure S51. Absorbance changes at 640 nm for 1:1 mixture of 5•Zn_2:PV (20 μM) upon addition of anions (0-10 equiv.).

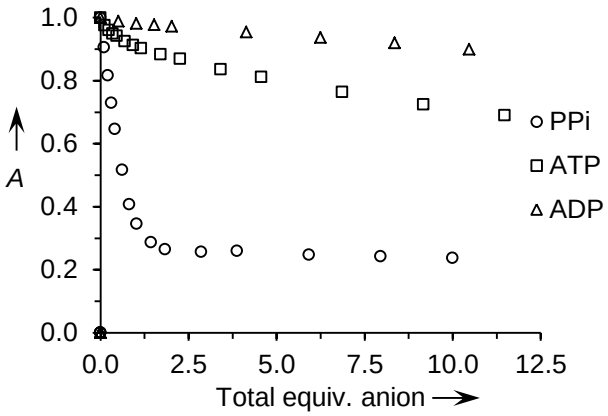

Figure S52. Absorbance changes at 600 nm for 1:1 mixture of 5•Zn_2:PR (20 μM) upon addition of anions (0-10 equiv.).

3.3.6 Receptor 6•Zn_2

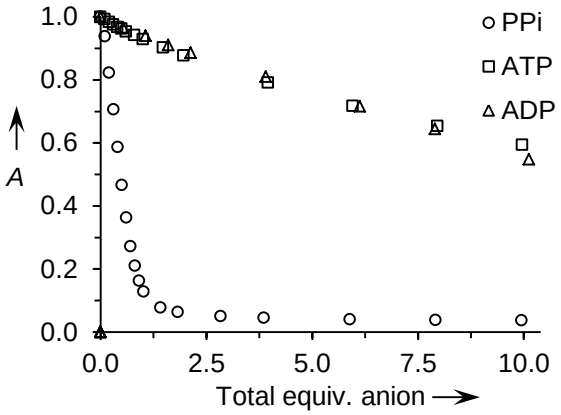

Figure S53. Absorbance changes at 640 nm for 1:1 mixture of 6•Zn_2:PV (20 μM) upon addition of anions (0-10 equiv.).

3.3.7 Receptor 7•Zn_2

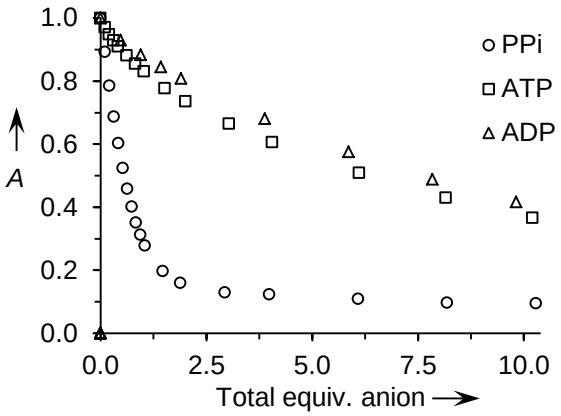

Figure S54. Absorbance changes at 640 nm for 1:1 mixture of 7•Zn_2:PV (20 μM) upon addition of anions (0-10 equiv.).

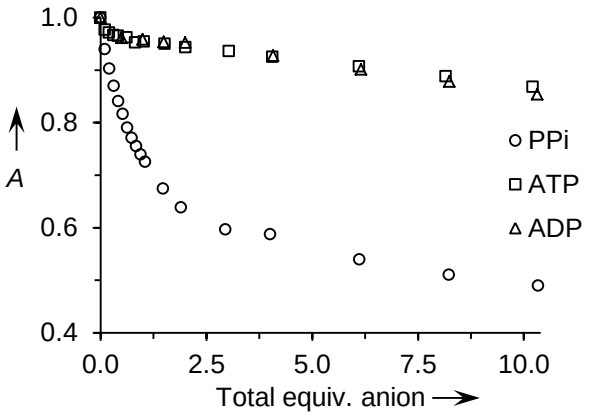

Figure S55. Absorbance changes at 600 nm for 1:1 mixture of 7•Zn_2:PR (20 μM) upon addition of anions (0-10 equiv.).

3.3.8 Receptor 8•Zn_2

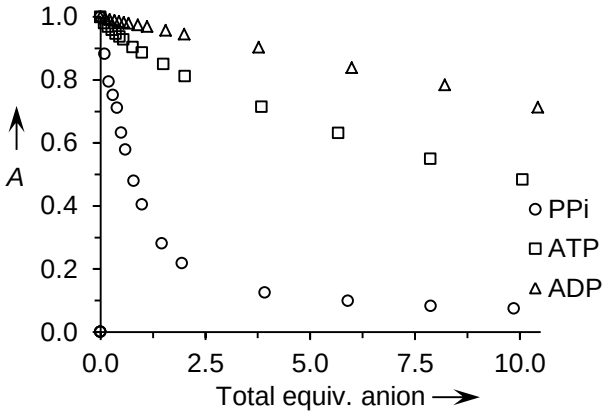

Figure S56. Absorbance changes at 640 nm for 1:1 mixture of 8•Zn_2:PV (20 μM) upon addition of anions (0-10 equiv.).

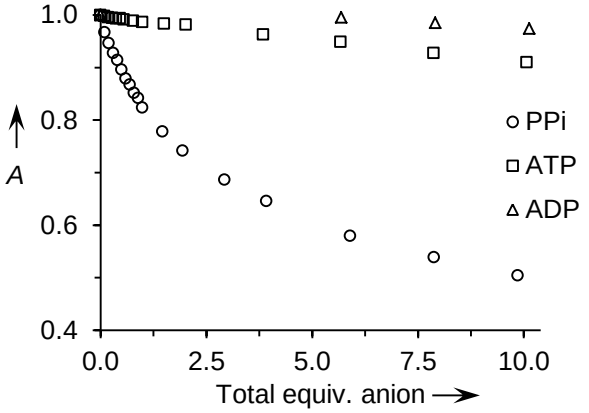

Figure S57. Absorbance changes at 600 nm for 1:1 mixture of 8•Zn_2:PR (20 μM) upon addition of anions (0-10 equiv.).

3.3.9 Receptor 9•Zn_2

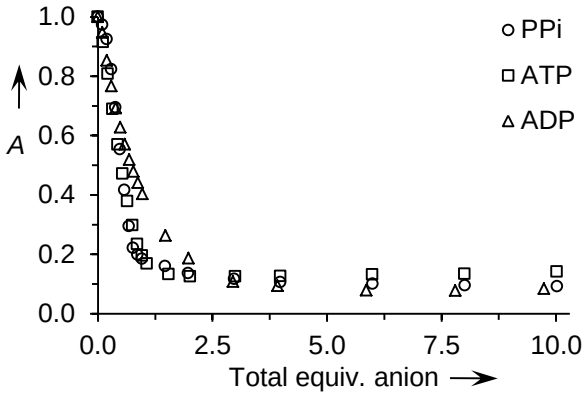

Figure S58. Absorbance changes at 640 nm for 1:1 mixture of 9•Zn_2:PV (20 μM) upon addition of anions (0-10 equiv.).

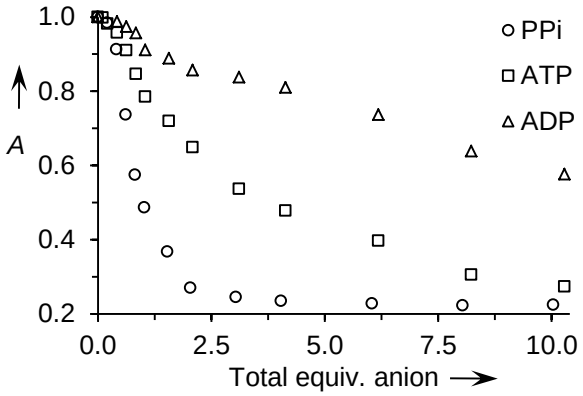

Figure S59. Absorbance changes at 600 nm for 1:1 mixture of 9•Zn_2:PR (20 μM) upon addition of anions (0-10 equiv.).

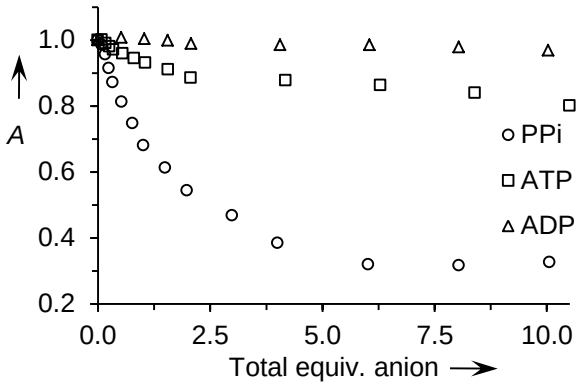

Figure S60. Absorbance changes at 610 nm for 1:1 mixture of 9•Zn_2:BPR (10 μM) upon addition of anions (0-10 equiv.).

4. Anion binding studies conducted in Kreb's buffer solution

4.1 Titrating indicator PV with complexes 1–7 and 9•Zn_2 in Kreb's buffer solution

Measurement conditions: aqueous solution of modified Kreb's buffer (137 mM NaCl, 5.4 mM KCl, 2.8 mM $CaCl_2$, 1.2 mM $MgSO_4$, 0.4 mM KH_2PO_4, 0.3 mM NaH_2PO_4, 10 mM glucose, 10 mM Tris-base, pH 7.4) at 25 °C.

Red lines indicate 1:1 stoichiometry (within experimental error) as determined using the mole ratio method.

4.1.1 Receptor 1•Zn_2

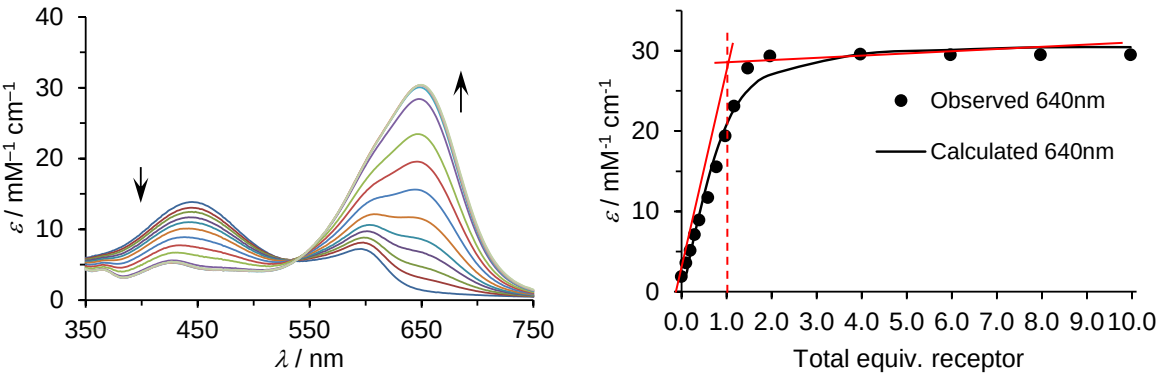

Figure S61. Left: Absorbance changes for PV solution (20 μM) upon addition of 1•Zn_2 (0-10 equiv.). Right: 1:1 fitting curve at 640 nm.

4.1.2 Receptor 2•Zn_2

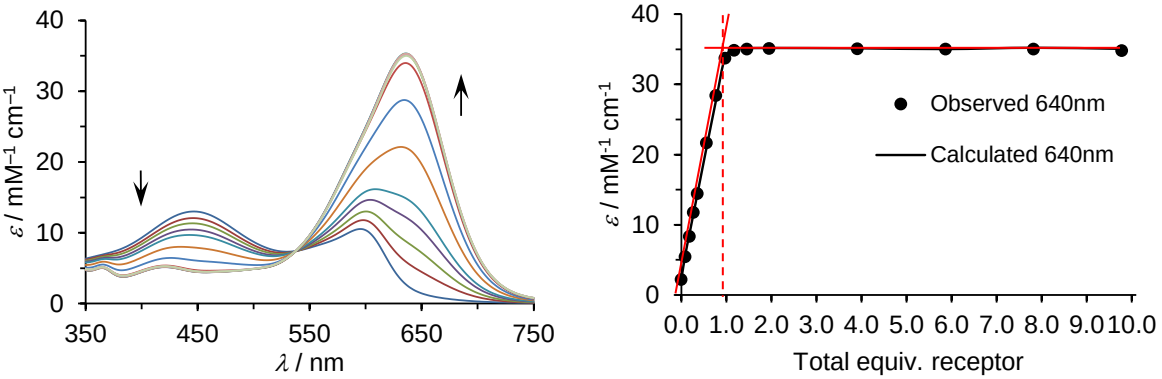

Figure S62. Left: Absorbance changes for PV solution (20 μM) upon addition of 2•Zn_2 (0-10 equiv.). Right: 1:1 fitting curve at 640 nm.

4.1.3 Receptor 3•Zn_2

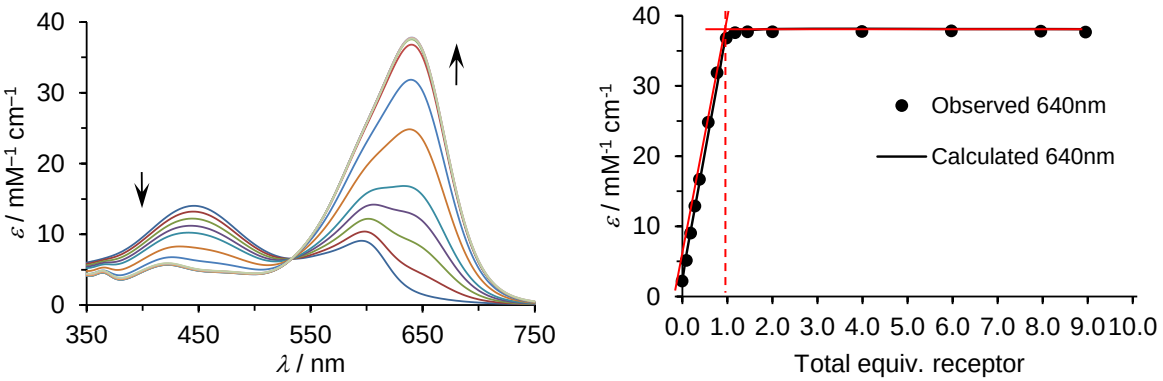

Figure S63. Left: Absorbance changes for PV solution (20 μM) upon addition of 3•Zn_2 (0-10 equiv.). Right: 1:1 fitting curve at 640 nm.

4.1.4 Receptor 4•Zn_2

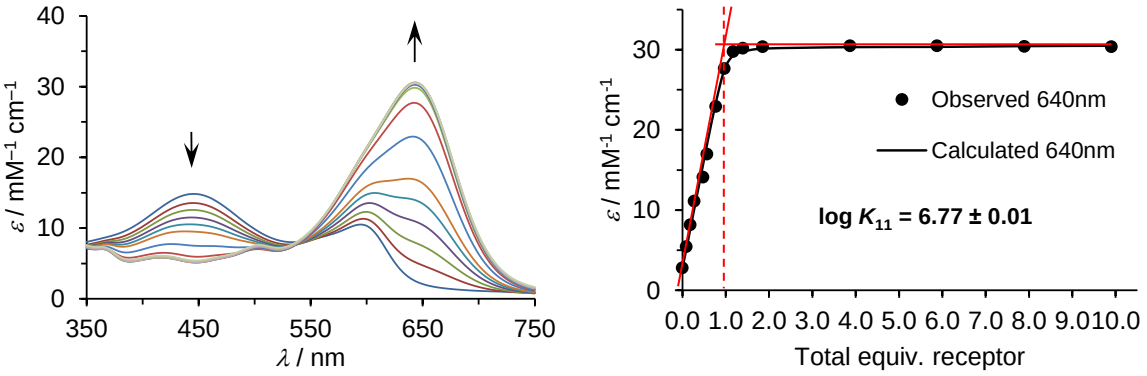

Figure S64. Left: Absorbance changes for PV solution (20 μM) upon addition of 4•Zn_2 (0-10 equiv.). Right: 1:1 fitting curve at 640 nm.

4.1.5 Receptor 5•Zn_2

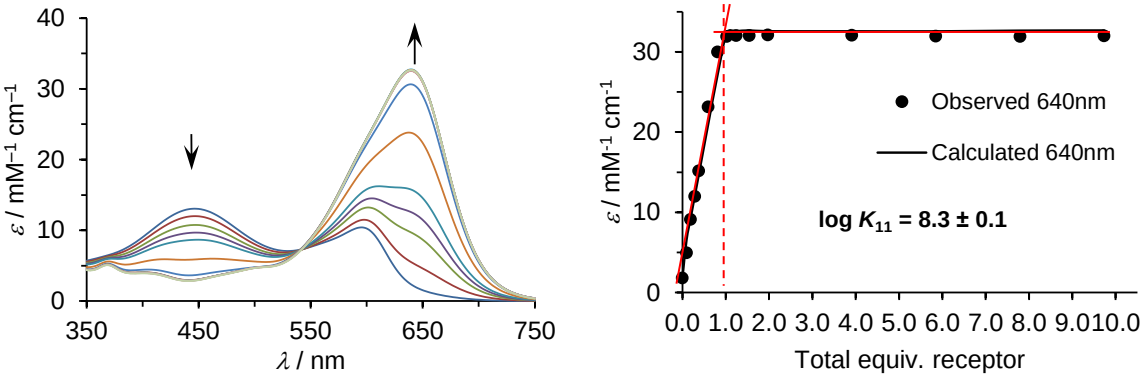

Figure S65. Left: Absorbance changes for PV solution (20 μM) upon addition of 5•Zn_2 (0-10 equiv.). Right: 1:1 fitting curve at 640 nm.

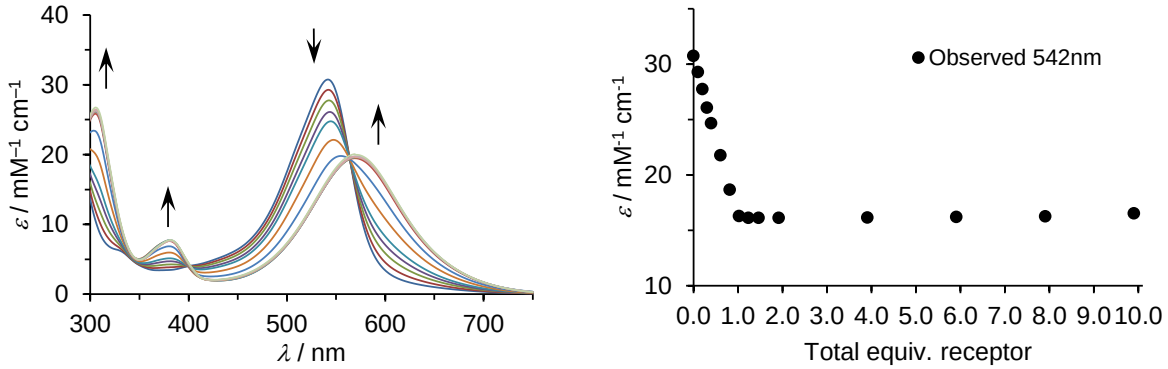

Figure S66. Left: Absorbance changes for PR solution (20 μM) upon addition of 5•Zn_2 (0-10 equiv.). Right: Absorbance at 542 nm, a satisfactory fitting curve was not obtained.

4.1.6 Receptor 6•Zn_2

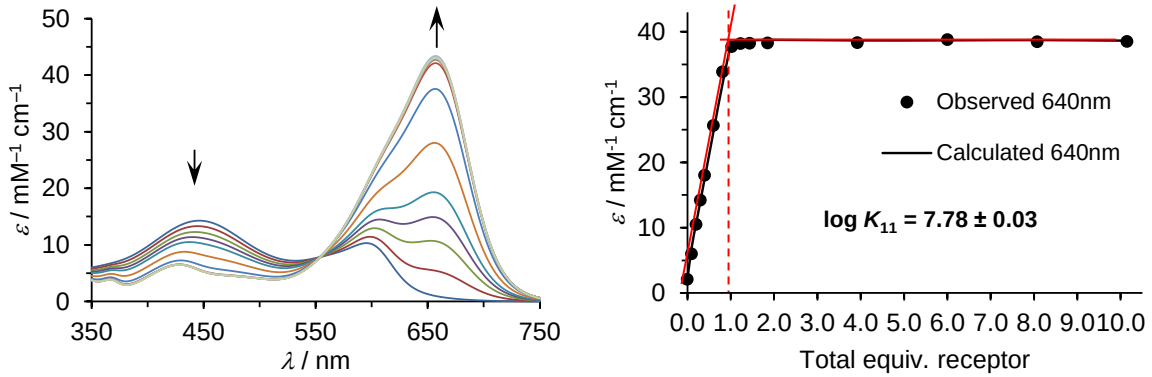

Figure S67. Left: Absorbance changes for PV solution (20 μM) upon addition of 6•Zn_2 (0-10 equiv.). Right: 1:1 fitting curve at 640 nm.

4.1.7 Receptor 7•Zn_2

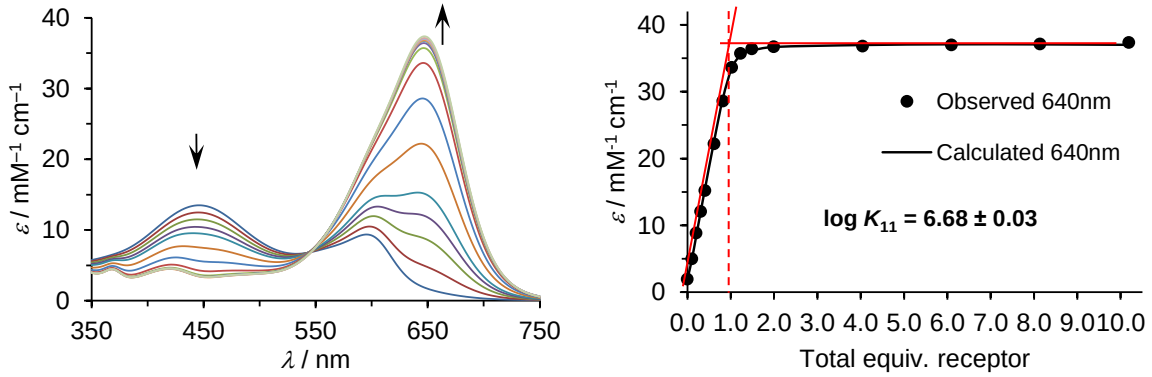

Figure S68. Left: Absorbance changes for PV solution (20 μM) upon addition of 7•Zn_2 (0-10 equiv.). Right: 1:1 fitting curve at 640 nm.

4.1.4 Receptor 9•Zn_2

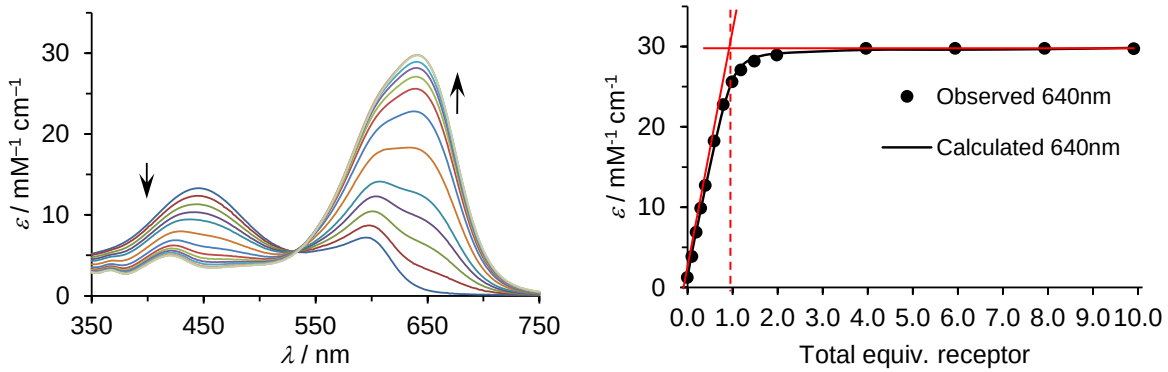

Figure S69. Left: Absorbance changes for PV solution (20 μM) upon addition of 9•Zn_2 (0-10 equiv.). Right: 1:1 fitting curve at 640 nm.

4.2 Titrating receptor-indicator ensembles with various anions in Kreb's buffer solution

Measurement conditions: aqueous solution of modified Kreb's buffer (137 mM NaCl, 5.4 mM KCl, 2.8 mM $CaCl_2$, 1.2 mM $MgSO_4$, 0.4 mM KH_2PO_4, 0.3 mM NaH_2PO_4, 10 mM glucose, 10 mM Tris-base, pH 7.4) at 25 °C. Anions are added as sodium salts.

4.2.1 Receptor 1•Zn_2

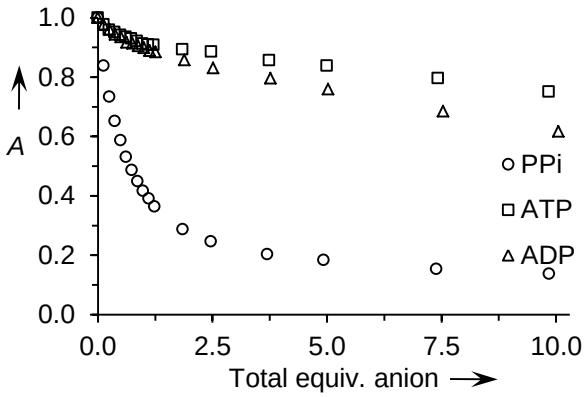

Figure S70. Absorbance changes at 640 nm for 1:1 mixture of 1•Zn_2:PV (20 μM) upon addition of anions (0-10 equiv.).

4.2.2 Receptor 2•Zn_2

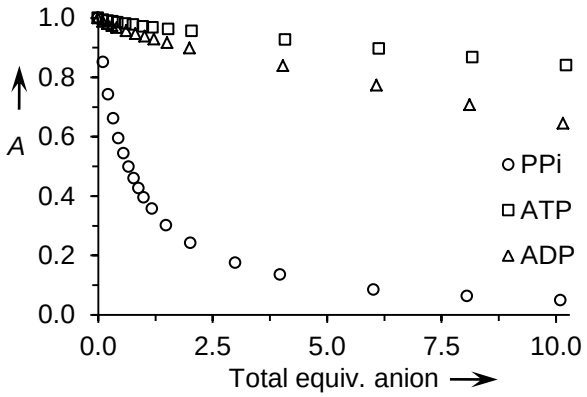

Figure S71. Absorbance changes at 640 nm for 1:1 mixture of 2•Zn_2:PV (20 μM) upon addition of anions (0-10 equiv.).

4.2.3 Receptor 3•Zn_2

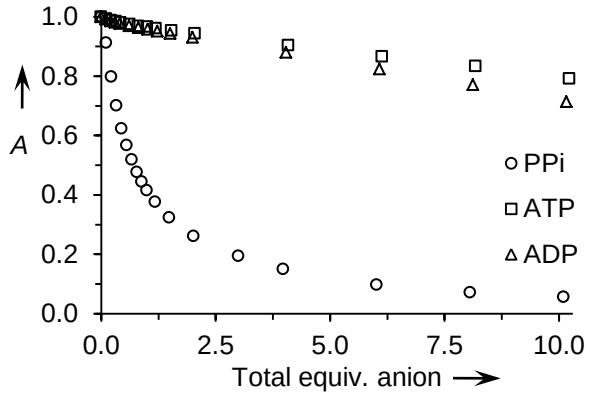

Figure S72. Absorbance changes at 640 nm for 1:1 mixture of 3•Zn_2:PV (20 μM) upon addition of anions (0-10 equiv.).

4.2.4 Receptor 4•Zn_2

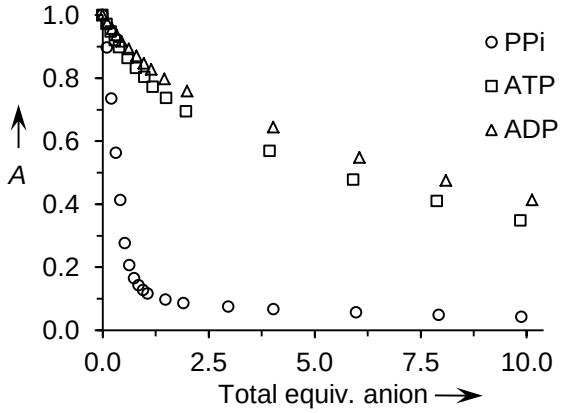

Figure S73. Absorbance changes at 640 nm for 1:1 mixture of 4•Zn_2:PV (20 μM) upon addition of anions (0-10 equiv.).

4.2.5 Receptor 5•Zn_2

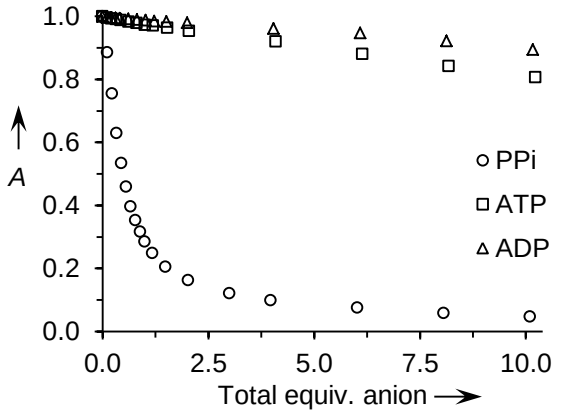

Figure S74. Absorbance changes at 640 nm for 1:1 mixture of 5•Zn_2:PV (20 μM) upon addition of anions (0-10 equiv.).

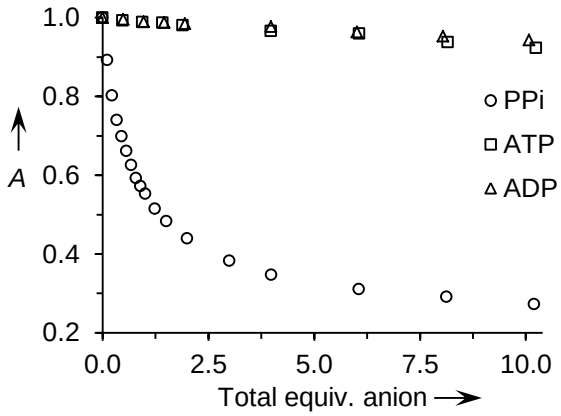

Figure S75. Absorbance changes at 542 nm for 1:1 mixture of 5•Zn_2:PR (20 μM) upon addition of anions (0-10 equiv.).

4.2.6 Receptor 6•Zn_2

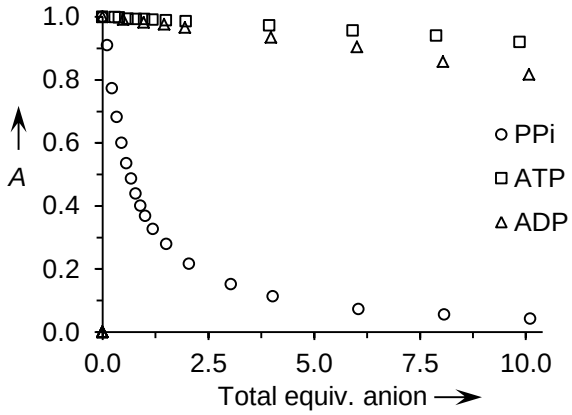

Figure S76. Absorbance changes at 640 nm for 1:1 mixture of 6•Zn_2:PV (20 μM) upon addition of anions (0-10 equiv.).

4.2.7 Receptor 7•Zn_2

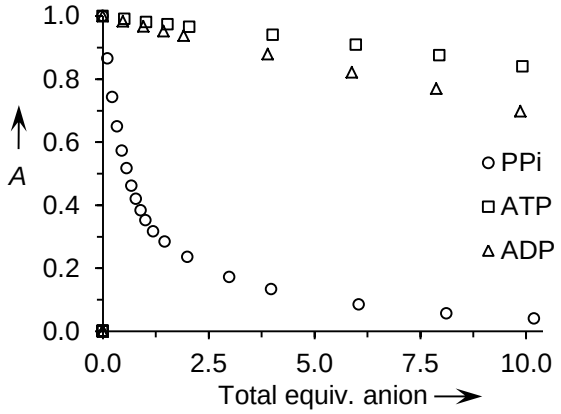

Figure S77. Absorbance changes at 640 nm for 1:1 mixture of 7•Zn_2:PV (20 μM) upon addition of anions (0-10 equiv.).

4.2.8 Receptor 9•Zn_2

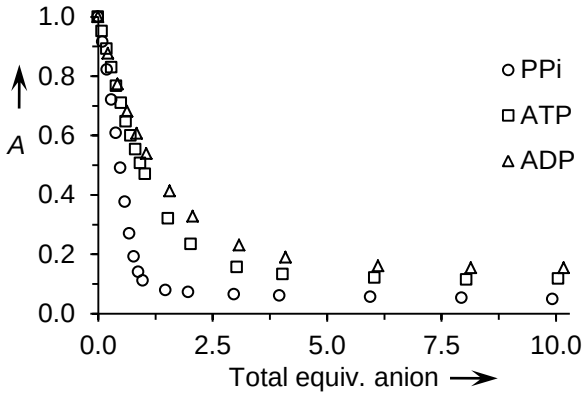

Figure S78. Absorbance changes at 640 nm for 1:1 mixture of 9•Zn_2:PV (20 μM) upon addition of anions (0-10 equiv.).

5. Colorimetric photos of receptor-indicator ensembles with various anions

Figure S79. The colors of the 1:1 mixtures of **2•Zn$_2$** (20 μM) and a) **PV**, b) **BPR** and c) **PR** with (from left): no anion, PPi, ATP, ADP, AMP, c-AMP, P-threonine, P-serine, P-tyrosine, HPO_4^{2-} and citrate (5 eq. each) in HEPES buffer (5 mM, 145 mM NaCl, pH 7.4).

6. Calibration curves for PPi

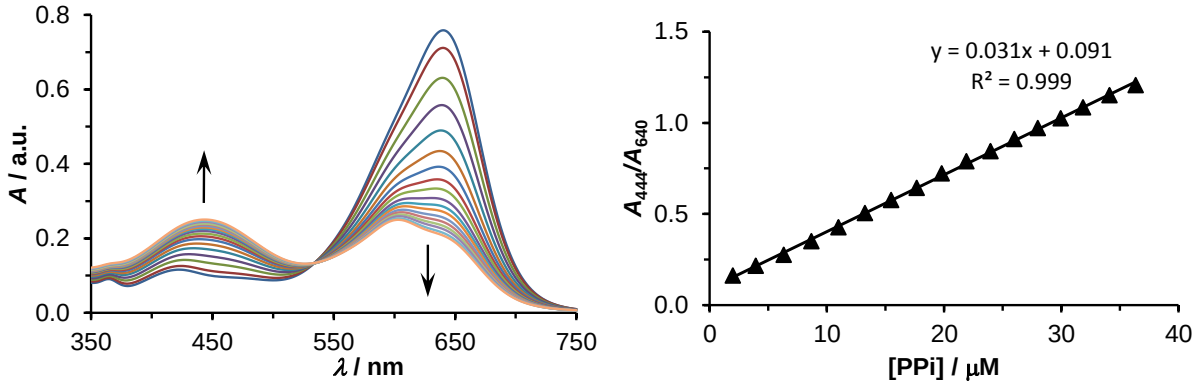

Figure S80. Left: Absorbance changes of **3•Zn$_2$:PV** ensemble (20 μM) upon the addition of **PPi** (0-36 μM). Right: Calibration curve for **PPi** based on ratiometric absorbances at 444 nm and 640 nm. Measurements were carried out in Kreb's buffer, pH 7.4 at 25 ^{o}C.

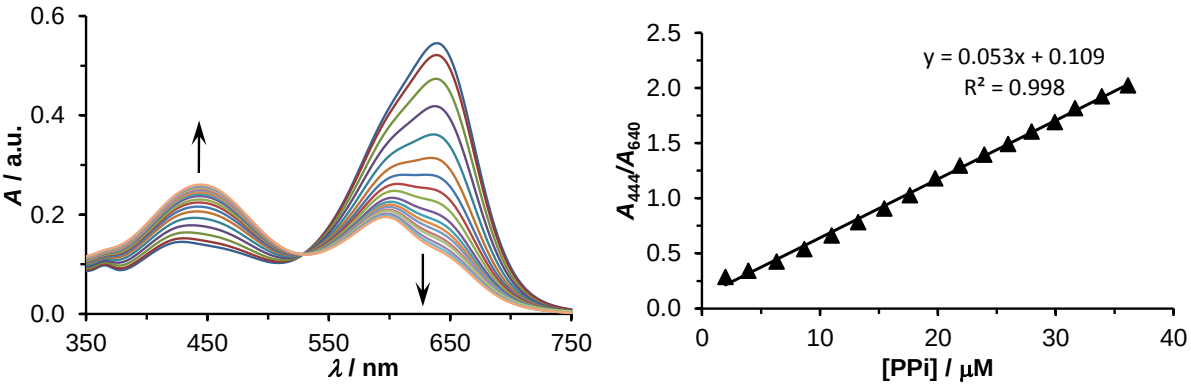

Figure S81. Left: Absorbance changes of **3•Zn_2:PV** ensemble (20 μM) upon the addition of **PPi** (0-36 μM) in the presence of **ATP** (250 μM). Right: Calibration curve for **PPi** based on ratiometric absorbances at 444 nm and 640 nm. Measurements were carried out in Kreb's buffer, pH 7.4 at 25 ^{o}C.

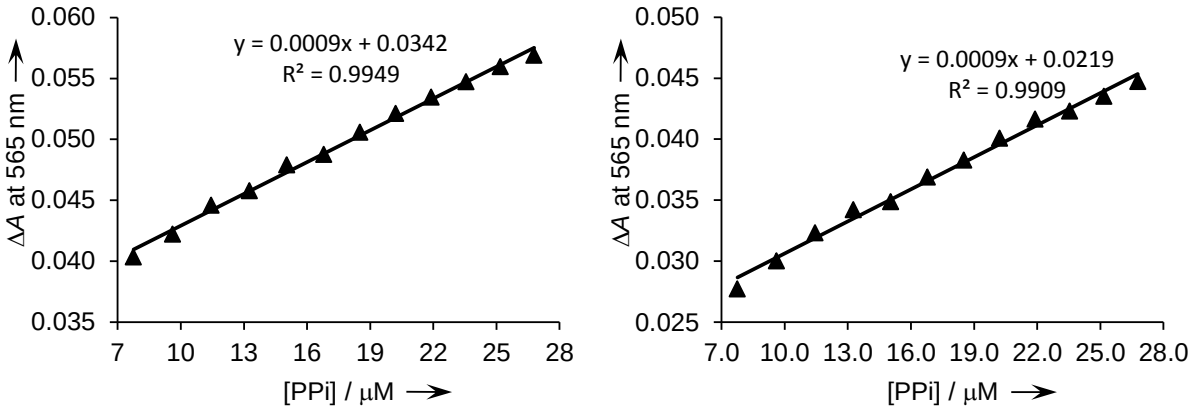

Figure S82. Left: Calibration curve for **PPi** based on absorbance changes at 565 nm of **2•Zn_2:PR** ensemble (20 μM) without ATP. Right: Calibration curve for **PPi** based on absorbance changes at 565 nm of **2•Zn_2:PR** ensemble (20 μM) in the presence of ATP (250 μM). Measurements were carried out in HEPES buffer (5 mM, pH 7.4, 145 mM NaCl) at 25 ^{o}C.

7. ^{1}H and ^{31}P NMR spectra for receptor 1•Zn_2 with PPi and ATP

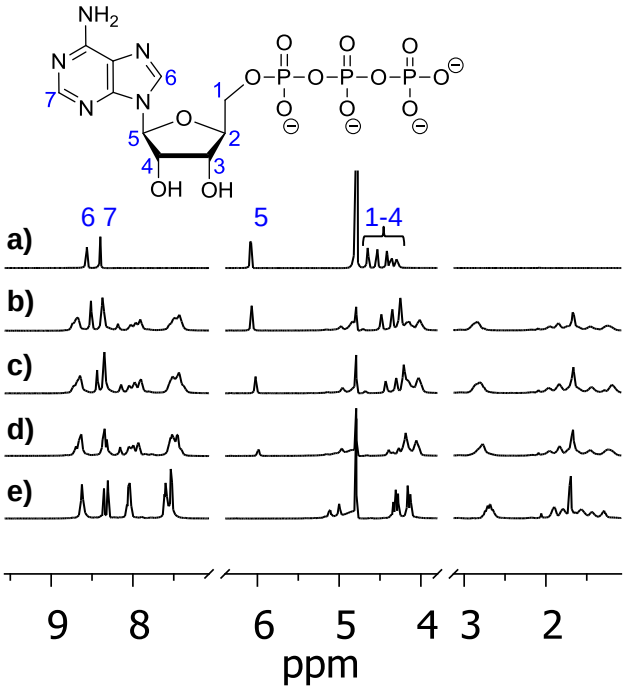

Figure S83. ^{1}H NMR (500 MHz) spectra of a) ATP alone, b) ATP:1•Zn_2 2:1, c) ATP:1•Zn_2 1:1, d) ATP:1•Zn_2 1:2 and e) 1•Zn_2 alone. All spectra were measured in D_2O at 300 K.

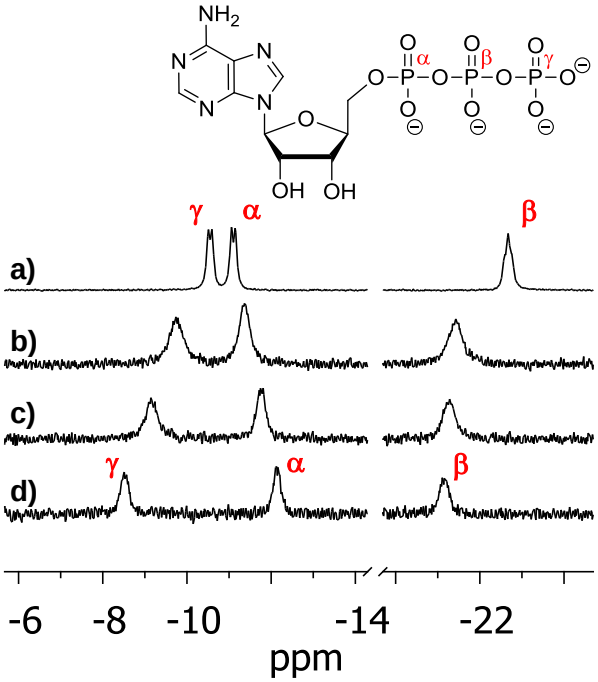

Figure S84. ^{31}P NMR (202 MHz) spectra of a) ATP alone, b) ATP:1•Zn_2 2:1, c) ATP:1•Zn_2 1:1 and d) ATP:1•Zn_2 1:2. All spectra were measured in D_2O at 300 K.

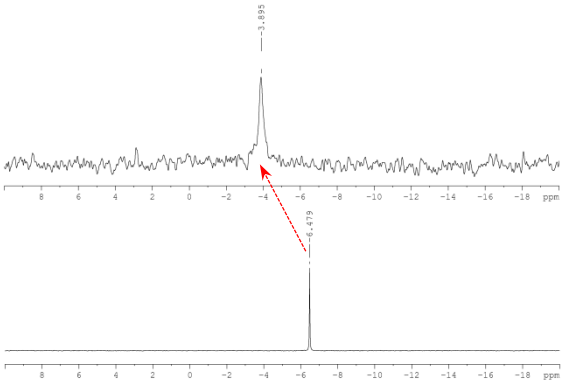

Figure S85. ^{31}P NMR (202 MHz) spectra of a) PPi alone and b) PPi:1•Zn_2 1:1. All spectra were measured in D_2O at 300 K.

8. References

1. S. J. Butler and K. A. Jolliffe, *Org. Biomol. Chem.*, 2011, 9, 3471-3483.
2. S. J. Butler, K. A. Jolliffe, W. Y. G. Lee, M. J. McDonough and A. J. Reynolds, *Tetrahedron*, 2011, 67, 1019-1029.
3. M. J. McDonough, A. J. Reynolds, G. W. Y. Lee and K. A. Jolliffe, *Chem. Commun.*, 2006, 2971-2973.
4. P. Gans, A. Sabatini and A. Vacca, *Talanta*, 1996, 43, 1739-1753.
5. K. A. Connors, *Binding Constants: The Measurement of Molecular Complex Stability*, John Wiley and Sons, New York, 1987.